QUANTITATIVE FINANCE
RESEARCH CENTRE

UNIVERSITY OF
TECHNOLOGY SYDNEY

QUANTITATIVE FINANCE RESEARCH CENTRE

Research Paper 394 October 2018, updated January 2019

Pricing American Options with Jumps in Asset and Volatility

Blessing Taruvinga, Boda Kang and Christina Sklibosios Nikitopoulos

ISSN 1441-8010 www.qfrc.uts.edu.au

Pricing American Options with Jumps in Asset and Volatility

Boda Kang[b], Christina Sklibosios Nikitopoulos[a], Blessing Taruvinga[a]

[a] *University of Technology Sydney,*
Finance Discipline Group, UTS Business School,
PO Box 123 Broadway NSW 2007, Australia
[b] *University of York, UK*
[c] *January 7, 2019*

Abstract

We numerically evaluate American call options under the Heston (1993) stochastic volatility model with asset and volatility jumps and the Hull and White (1987) short rate model. By employing the Method of Lines (Meyer (2015)), the option price, the early exercise boundary and the Greeks are computed as part of the solution, which makes the numerical implementation time efficient. We conduct a numerical study to gauge the impact of jumps and stochastic interest rates on American call option prices and on their free boundaries. Jumps tend to increase the values of OTM and ATM options while decreasing the value of ITM options. The option delta is affected in a similar way. The impact of jumps on the free boundary is substantial and depends on the time to maturity. Far from expiry, including asset jumps lowers the free boundary and the option holder is more likely to exercise the option, whilst including asset-volatility jumps elevates the free boundary and the option holder is less likely to exercise the option. This relation reverses at the end of the options life. The volatility, interest rates and their volatilities have a positive impact on the free boundaries and the option holder is less likely to exercise as these parameters increase.

Keywords: American options; Method of Lines; stochastic interest rate; Jumps; Greeks
JEL: C60, G13

*Corresponding author
Email addresses: Boda.Kang@uts.edu.au (Boda Kang), christina.nikitopoulos@uts.edu.au (Christina Sklibosios Nikitopoulos), Blessing.Taruvinga@student.uts.edu.au (Blessing Taruvinga)

1. Introduction

Numerous approaches have been proposed in the literature to relax the Black and Scholes (1973) model assumptions for pricing European options in order to create more realistic models which reflect the behavior of market prices, for example by including features such as stochastic volatility, stochastic interest rates, jump diffusion and combinations thereof. For example, stochastic volatility models capture the empirically observed leptokurtosis in the markets, stochastic interest rates improve pricing and hedging of long-dated contracts, jump-diffusions tend to explain better shorter maturity smiles, etc.[1]

Another extension of practical importance is the pricing of American options, taking into account the fact that many options traded in the market have early exercise features. From the seminal paper by Black (1975), many numerical applications have been considered in the literature to value options featuring early exercise, in addition to stochastic volatility, stochastic interest rates and jumps. There have been several papers which discuss the assumption of stochastic volatility in pricing American options, including Clarke and Parrott (1999), Ikonen and Toivanen (2009), Beliaeva and Nawalkha (2010), Haentjens and int Hout (2015) and Agarwal et al. (2016). The early exercise premium for American options at any time before maturity depends on the term structure of interest rates (i.e. Ho et al. (1997)), thus interest rate volatility cannot be ignored especially for long term options. Amin and Bodurtha (1995), Chung (1999) and Detemple and Tian (2002) price American options under the assumption of stochastic interest rates. Some American option pricing models combine both stochastic volatility and stochastic interest rates, i.e. Medvedev and Scaillet (2010), Chiarella and Kang (2011), Kang and Meyer (2014).

[1]Representative literature on pricing European options with stochastic volatility models include Hull and White (1987), Stein and Stein (1991), Heston (1993), Schobel and Zhu (1999), etc. Stochastic interest rate models have been developed by Merton (1973), Amin and Jarrow (1992), Rindell (1995), Haowen (2012), Abudy and Izhakian (2013), etc., and combinations with stochastic volatility include the models by Kaushik I. Amin (1993), Grzelak et al. (2012), Haentjens and int Hout (2012), Guo et al. (2013), etc. Jump-diffusion models have been considered by Scott (1997), Bakshi et al. (1997), Doffou and Hilliard (2001), Kou (2002), Pan (2002), Kangro et al. (2003), Pinkham and Sattayatham (2011), Makate and Sattayantham (2011), Hua et al. (2012), Zhang and Wang (2013), Zhang and Wang (2013).

Extensions to accommodate jump diffusions have also been considered in the American option pricing literature. These typically help to explain the shorter maturity smiles. Bates (1996) developed a method for pricing American options for stochastic volatility/jump diffusion processes under systematic jump and volatility risk. According to Bates (1996), Bakshi et al. (1997) and Pan (2002), models with jumps in asset dynamics only are not capable of fully capturing the empirical features of equity index returns or option prices. They propose including jumps in the stochastic volatility and provide empirical evidence that models with only diffusive stochastic volatility and jumps in returns are misspecified, as they do not have a component driving the conditional volatility of returns, which is rapidly moving. Duffie et al. (2000) focused on an affine jump diffusion model which allows for correlated jumps in both volatility and price. They found that the level of skewness produced by including negative jumps does not fully reflect market data. According to Duffie et al. (2000) and Pan (2002), jumps in volatility increase the Black-Scholes implied volatility for in the money options and they labeled this as the "hook" or "tipping at the end" effect. A comprehensive description on the impact of jumps in both return and volatility dynamics is given by Eraker et al. (2003). They demonstrate that inclusion of jumps in returns helps to explain the large movements in the option prices whilst the inclusion of jumps in volatility allow it to increase rapidly, as jumps in returns are a rapidly moving but persistent factor driving volatility. Further, in comparison to stochastic volatility models, models with jumps in returns steepen the slope of the implied volatility, while adding another jump to volatility further steepens this slope. Boyarchenko and Levendorski (2007) priced American options in Levy models with stochastic interest rate of CIR type using an iteration method based on the Wiener-Hopf factorization, while Lamberton and Mikou (2008) looked at the behavior of American put option prices in the presence of asset jumps. More recent developments on models with asset and volatility jumps include Durhama and Park (2013) and Salmi et al. (2014). Itkin (2016) considers the pricing and hedging of exotic options whose dynamics include correlated jumps in asset, volatility and interest rates. The literature on evaluating with jumps in asset and volatility while assuming stochastic interest rates is rather limited. The current paper aims to make a contribution to this stream of literature.

In the absence of closed form solutions for options featuring early exercise, a variety

of numerical methods have been proposed to price these type of options, such as finite difference methods, splitting methods, multi-grid methods, numerical approximations, etc. Barone-Adesi and Whaley (1987) used an analytic approximation for pricing exchange traded American options on commodities and the futures contracts. They found their method to be accurate and more computationally efficient in comparison to other methods, i.e. binomial methods and finite difference methods. Broadie and Detemple (1996) propose price approximations with one based on the lower bound and the other based on both the lower and upper bounds. Both these methods were based on the Black-Scholes model. As the Black Scholes model was improved to incorporate stochastic volatility, stochastic interest rates and jumps, other methods such as binomial methods, Monte Carlo methods, finite difference methods have been used. Broadie and Glasserman (1997) priced American options using a simulation algorithm that has an advantage over lattice and finite difference methods when there are many state variables. Carriere (1996), Tsitsiklis and Roy (1999) and Longstaff and Schwartz (2001) also use simulation based techniques for this purpose, with the latter paper being most commonly referenced when pricing American options by Monte Carlo. Sullivan (2000) used Gaussian Quadrature together with Chebyshev approximation to price American put options, an alternative method to binomial models. Ikonen and Toivanen (2009) priced American options using five finite difference based methods, namely, the projected SOR, projected multigrid method, an operator splitting method, a penalty method and component-wise splitting method under the Heston model in order to check the speed and the accuracy of these methods. Agarwal et al. (2016) combined finite difference methods and Monte Carlo to price American options with stochastic volatility.

This paper evaluates American call options with stochastic volatility and stochastic interest rate models that allow for asset and volatility jumps. The proposed model assumes Heston (1993) volatility dynamics and Hull and White (1990) type dynamics for the interest rates. The asset jumps part is a compound Poisson process which consists of a random variable and a Poisson process, and is independent from the continuous part. The jump sizes are log-normally distributed, see Merton (1976), Kangro et al. (2003), Chiarella et al. (2009). The volatility jump size is exponentially distributed in order to ensure that the variance jumps are not negative, as normally observed after large downward jumps occur in

asset prices (Lutz (2010)).

For the numerical evaluations of American call options under these model assumptions, we employ the Method of Lines (MoL hereafter) algorithm due to its accuracy and numerical efficiency, see Meyer (1998). The MoL for pricing American options was used by Meyer and van der Hoek (1997) with the asset price process following a diffusion process. Extensions to jump diffusion with the MoL were discussed in Meyer (1998). Chiarella et al. (2009) evaluate American options under the assumption that asset price dynamics are driven by the jump diffusion process proposed by Merton (1976), and the volatility follows the square root process by Heston (1993). They also demonstrated the computational efficiency of the MoL compared to componentwise splitting and Crank-Nicholson methods. The MoL was also used by Chiarella and Ziveyi (2011) to price American options with two stochastic volatility processes, Adolfsson et al. (2013) to price American call option under Heston stochastic volatility dynamics, Kang and Meyer (2014) to price American options whose dynamics include stochastic interest rate of the CIR type and Chiarella et al. (2016) to price American options under regime switching. In this paper, we apply the MoL to numerically solve the American call option pricing problem under stochastic volatility, stochastic interest rates and jumps in both asset prices and volatility.

The remainder of the paper is structured as follows. Section 2 describes the pricing model for American call options, which allows for stochastic volatility, stochastic interest rates and jumps in both the asset and the volatility and derives the corresponding PIDE pricing equation. The implementation details of the MoL algorithm are included in Section 3. Section 4 confirms the accuracy of the MoL implementation and presents a sensitivity analysis to gauge the impact of stochastic volatility and stochastic interest rates on the free boundary surfaces. Section 5 assess the impact of asset and volatility jumps on American call prices, their free boundaries and Greeks. Section 6 concludes.

2. American Call Option Pricing: The Valuation Model

This section describes the model used to price American call options. In line with the model of Duffie et al. (2000), which includes jumps in both the asset and volatility dynamics, the Heston (1993) stochastic volatility model with asset and volatility jumps is considered.

The interest rate process follows the Hull and White (1987) interest rate model. Thus, under the risk-neutral measure $\mathbb{Q}$, the dynamics of the underlying price are given by the following equations:

$$\begin{aligned} dS &= (r - q - \lambda_1 k)\, S dt + \sqrt{V} S dZ_1 + (Y-1)\, S dN_1, \\ dV &= \kappa\,(\theta - V)\, dt + \sigma_V \sqrt{V} dZ_2 + y dN_2, \\ dr &= a\,(b\,(t) - r)\, dt + \sigma_r dZ_3, \end{aligned} \tag{1}$$

where S is the stock price, r is the instantaneous interest rate whose dynamics are given by the Hull and White (1987) model, q is continuously compounded dividend rate, V is the variance process, Z_i (for $i = 1,\ 2,\ 3$) is a standard Wiener process under the risk-neutral measure $\mathbb{Q}$, $Y - 1$ is the random variable percentage change in the asset price if a jump occurs, dN_i is a Poisson increment, which is given by:

$$dN_i = \begin{cases} 1, & \text{with probability } \ \lambda_i dt, \\ 0, & \text{with probability } \ 1 - \lambda_i dt, \qquad \text{for } i = 1, 2 \end{cases}$$

where dN_1 and dN_2 are jump processes with jump intensities λ_1 and λ_2 respectively. They are not correlated and are also independent from the continuous part of the process (Lutz (2010)),

$$k = E^{\boldsymbol{Q}}\,(Y-1) = \int_0^\infty (Y-1)\, G\,(Y)\, dY, \tag{2}$$

where $G\,(Y)$ is the probability distribution of Y under the risk-neutral measure $\mathbb{Q}$, κ is the rate of mean reversion of V, θ is the long run mean of V, σ_V is the instantaneous volatility of V, y is the absolute jump size of the volatility process, a is the rate of mean reversion of r, $b\,(t)$ is the long run mean of r which is given as

$$b\,(t) = c_1 - c_2 e^{-c_3 t} \tag{3}$$

where c_1, c_2 and c_3 are positive constants and $c_1 > c_2$, σ_r is the instantaneous volatility of r. In order for the variance process to remain positive, $\kappa, \theta,$ and σ_V will have to be selected such that the following Feller condition (Feller (1951)) is satisfied

$$2\kappa\theta > \ \sigma_V^2.$$

The correlation structure between the Wiener processes under the risk-neutral measure $\mathbb{Q}$ is assumed to be given by

$$E^{\boldsymbol{Q}}\left(dZ_1 dZ_2\right) = \rho_{12}dt, E^{\boldsymbol{Q}}\left(dZ_1 dZ_3\right) = \rho_{13}dt, E^{\boldsymbol{Q}}\left(dZ_2 dZ_3\right) = \rho_{23}dt,$$

where $\rho_{i,j}$ for $i = 1, 2$ and $j = 2, 3$ are constants.

2.1. Partial integro-differential equation (PIDE) derivation using the Martingale approach

The system of correlated Wiener processes (1) is transformed to a system of uncorrelated Wiener processes using Cholesky decomposition, as it is more convenient to work with a system of independent Wiener processes. The resulting system of independent Wiener processes W_1, W_2, and W_3 is given below as:

$$\begin{aligned}
dS &= \left(r - q - \lambda_1 k\right) S dt + \sqrt{V} S dW_1 + \left(Y - 1\right) S dN_1, \\
dV &= \kappa\left(\theta - V\right) dt + \sigma_V \sqrt{V}\rho_{12} dW_1 + \sigma_V \sqrt{V}\left(1 - \rho_{12}^2\right)^{\frac{1}{2}} dW_2 + y dN_2, \\
dr &= a\left(b\left(t\right) - r\right) dt + \sigma_r \rho_{13} dW_1 + \sigma_r \frac{\rho_{32} - \rho_{12}\rho_{13}}{\sqrt{1 - \rho_{12}^2}} dW_2 \\
&\quad + \sigma_r \left(\frac{1 - \rho_{12}^2 - \rho_{13}^2 - \rho_{23}^2 + 2\rho_{12}\rho_{13}\rho_{23}}{1 - \rho_{12}^2}\right)^{\frac{1}{2}} dW_3.
\end{aligned} \tag{4}$$

The infinitesimal generator $\boldsymbol{K}$ of this system of equations is given as:

$$\begin{aligned}
\boldsymbol{K} &= \left(r - q - \lambda_1 k\right) S \frac{\partial}{\partial S} + \kappa\left(\theta - V\right) \frac{\partial}{\partial V} + a\left(b\left(t\right) - r\right) \frac{\partial}{\partial r} + VS^2 \frac{1}{2} \frac{\partial^2}{\partial S^2} + \sigma_V^2 V \frac{1}{2} \frac{\partial^2}{\partial V^2} \\
&\quad + \sigma_r^2 \frac{1}{2} \frac{\partial^2}{\partial r^2} + VS\sigma_V \rho_{12} \frac{\partial^2}{\partial S \partial V} + \sqrt{V} S \sigma_r \rho_{13} \frac{\partial^2}{\partial S \partial r} + \sigma_r \sigma_V \sqrt{V} \rho_{23} \frac{\partial^2}{\partial V \partial r} \\
&\quad + \lambda_1 \int \left(f\left(YS, t\right) - f\left(S, t\right)\right) G\left(Y\right) dY + \lambda_2 \int \left(f\left(V + y, t\right) - f\left(V, t\right)\right) g\left(y\right) dy,
\end{aligned} \tag{5}$$

where $g\left(y\right)$ is the probability distribution of y under the risk-neutral measure $\mathbb{Q}$. Let $f\left(t, S, V, r\right)$ be the price of an option with maturity T at time t. Option pricing can be performed under an equivalent martingale measure which is determined by its numeraire. Under the risk-neutral probability measure $\mathbb{Q}$, the current option value is computed by the expected discounted future payoff of the option, since the option price denominated at the money market account is a Martingale under the risk-neutral measure. Mathematically:

$$f\left(t, S, V, r\right) = \boldsymbol{E}_t^{Q}\left[e^{-\int_t^T r(s)ds} f\left(T, S, V, r\right)\right]$$

The Feynman-Kac formula states that $f(t,S,V,r)$ satisfies the integro partial differential equation:

$$\frac{\partial f}{\partial t}+\mathbf{K}f-rf=0,$$

subject to the initial condition

$$\lim_{t\to T} f(t,S,V,r)=f(T,S,V,r).$$

Hence the PIDE that need to be solved to obtain the option price is given as:

$$\begin{aligned}&\frac{\partial f}{\partial t}+(r-q-\lambda_1 k)S\frac{\partial f}{\partial S}+\kappa(\theta-V)\frac{\partial f}{\partial V}+a(b(t)-r)\frac{\partial f}{\partial r}+VS^2\frac{1}{2}\frac{\partial^2 f}{\partial S^2}+\sigma_V^2 V\frac{1}{2}\frac{\partial^2 f}{\partial V^2}\\&+\sigma_r^2\frac{1}{2}\frac{\partial^2 f}{\partial r^2}+VS\sigma_V\rho_{12}\frac{\partial^2 f}{\partial S\partial V}+\sqrt{V}S\sigma_r\rho_{13}\frac{\partial^2 f}{\partial S\partial r}+\sigma_r\sigma_V\sqrt{V}\rho_{23}\frac{\partial^2 f}{\partial V\partial r}-rf\\&+\lambda_1\int(f(YS,t)-f(S,t))G(Y)\,dY+\lambda_2\int(f(V+y,t)-f(V,t))g(y)\,dy=0.\end{aligned}\tag{6}$$

Heston (1993) included the term $\lambda_V(t,S,V)$ in the partial differential equation to represent the price of volatility risk. In motivating the choice of $\lambda_V(t,S,V)$ he applies the consumption model by Breeden (1976) and obtains a price of volatility risk, which is a linear function of volatility, i.e. $\lambda_V(t,S,V)=\lambda_V V$.

Lamoureux and Lastrapes (1993) then investigated whether volatility risk does affect the option price. They tested whether the strong assumption of market indifference to volatility risk is consistent with data. They concluded that further attempts to learn from the data should explicitly model a risk premium on the variance process as given in the model by Heston (1993). As the model also includes the stochastic interest rate, interest rate risk $\lambda_r r$ is priced in line with Kang and Meyer (2014). Let time to maturity, τ be defined as $\tau=T-t$. Hence, the PIDE is given as:

$$\begin{aligned}&(r-q-\lambda_1 k)S\frac{\partial f}{\partial S}+(\kappa(\theta-V)-\lambda_V V)\frac{\partial f}{\partial V}+((a(b(\tau)-r))-\lambda_r r)\frac{\partial f}{\partial r}+VS^2\frac{1}{2}\frac{\partial^2 f}{\partial S^2}\\&+\sigma_V^2 V\frac{1}{2}\frac{\partial^2 f}{\partial V^2}+\sigma_r^2\frac{1}{2}\frac{\partial^2 f}{\partial r^2}+VS\sigma_V\rho_{12}\frac{\partial^2 f}{\partial S\partial V}+\sqrt{V}S\sigma_r\rho_{13}\frac{\partial^2 f}{\partial S\partial r}+\sigma_r\sigma_V\sqrt{V}\rho_{23}\frac{\partial^2 f}{\partial V\partial r}\\&+\lambda_1\int(f(YS,\tau)-f(S,\tau))G(Y)\,dY+\lambda_2\int(f(V+y,\tau)-f(V,\tau))g(y)\,dy-rf=\frac{\partial f}{\partial \tau}.\end{aligned}\tag{7}$$

2.2. The partial-integro differential equation for a call option and boundary conditions

Let the time to maturity, τ be defined as $\tau = T - t$. Let C, a function of τ, S, V, r be the American call option price given by $C(\tau, S, V, r)$. Then:

$$C(\tau, S, V, r) = \mathbf{E}_{\tau}^{Q}\left[e^{-\int_0^{\tau} r(s)ds} C(\tau, S, V, r)\right].$$

Using the Feynman-Kac formula $C(\tau, S, V, r)$ satisfies the integro partial differential equation:

$$\mathbf{K}C - rC = \frac{\partial C}{\partial \tau},$$

in the region

$$0 \leq \tau \leq T, \quad 0 < S \leq d(\tau, V, r), \quad 0 < V < \infty, \quad -\infty < r < \infty,$$

where $d(V, r, \tau)$ is the early exercise boundary, subject to the initial condition

$$\lim_{\tau \to 0} C(\tau, S, V, r) = C(\tau, S, V, r).$$

The domain for r includes negative interest rates since the Hull-White model allows for negative rates. At the free boundary point, the value matching condition

$$C(\tau, d(\tau, V, r), V, r) = d(\tau, V, r) - K,$$

must be satisfied as it ensures continuity of the option value function at the free boundary. To maximise the value of the American call option and avoid arbitrage in the model , the following smooth pasting conditions need to be included at the free boundary:

$$\lim_{S \to d(\tau,V,r)} \frac{\partial C}{\partial S} = 1, \quad \lim_{S \to d(\tau,V,r)} \frac{\partial C}{\partial V} = 0, \quad \lim_{S \to d(\tau,V,r)} \frac{\partial C}{\partial r} = 0. \tag{8}$$

This condition implies that the American call option value is maximised by a strategy that makes the value of the option and the delta of the option continuous. The computational domain is

$$0 \leq \tau \leq T, \quad S_{\min} < S \leq S_{\max}, \quad V_{\min} < V < V_{\max}, \quad -r_{\min} < r < r_{\max}. \tag{9}$$

Meyer (2015) used the MoL in pricing a call option under the Heston-Hull-White model. On imposing conditions on the boundary with negative interest rates based on the Black-Scholes formula, he found that they were not consistent with the behaviour of an American call option, and, as a result, only the positive domain for interest rates was considered. Similar considerations shall be made in this paper.

Following the results obtained previously, the PIDE that needs to be solved to obtain the option price is

$$\begin{aligned}
&(r-q-\lambda_1 k)\, S\frac{\partial C}{\partial S} + (\kappa(\theta - V) - \lambda_V V)\frac{\partial C}{\partial V} + ((a(b(\tau) - r)) - \lambda_r r)\frac{\partial C}{\partial r} + VS^2\frac{1}{2}\frac{\partial^2 C}{\partial S^2} \\
&+ \sigma_V^2 V\frac{1}{2}\frac{\partial^2 C}{\partial V^2} + \sigma_r^2\frac{1}{2}\frac{\partial^2 C}{\partial r^2} + VS\sigma_V\rho_{12}\frac{\partial^2 C}{\partial S\partial V} + \sqrt{V}S\sigma_r\rho_{13}\frac{\partial^2 C}{\partial S\partial r} + \sigma_r\sigma_V\sqrt{V}\rho_{23}\frac{\partial^2 C}{\partial V\partial r} - rC \\
&+ \lambda_1\int (C(YS,\tau) - C(S,\tau))\, G(Y)\, dY + \lambda_2\int (C(V+y,\tau) - C(V,\tau))\, g(y)\, dy = \frac{\partial C}{\partial \tau}.
\end{aligned} \tag{10}$$

The boundary conditions at the points S_{min}, S_{max}, V_{min}, V_{max}, r_{min} and r_{max} are discussed below. At $S = S_{max}$, the value of the call option is

$$C(\tau, S_{max}, V, r) = S_{max} - K.$$

To determine the type of boundary conditions to be used at $S = 0$, $V = 0$ and $r = 0$, Meyer (2015) and Kang and Meyer (2014) use the algebraic sign of the Fichera function for the PIDE. Applying these results, the option price at $S = 0$ is

$$C(\tau, 0, V, r) = 0.$$

At the point $V = 0$, the PIDE becomes

$$\begin{aligned}
&\sigma_r^2\frac{1}{2}\frac{\partial^2 C}{\partial r^2} + (r-q-\lambda_1 k)\, S\frac{\partial C}{\partial S} + \kappa\theta\frac{\partial C}{\partial V} + ((a(b(\tau) - r)) - \lambda_r r)\frac{\partial C}{\partial r} - rC \\
&+ \lambda_1\int (C(YS,\tau) - C(S,\tau))\, G(Y)\, dY + \lambda_2\int (C(y,\tau) - C(0,\tau))\, g(y)\, dy = \frac{\partial C}{\partial \tau},
\end{aligned} \tag{11}$$

and at $r = 0$ the PIDE reduces to

$$
\begin{aligned}
&(r-q-\lambda_1 k)\, S\frac{\partial C}{\partial S} + (\kappa(\theta - V) - \lambda_V V)\frac{\partial C}{\partial V} + a(b(\tau))\frac{\partial C}{\partial r} \\
&+ VS^2\frac{1}{2}\frac{\partial^2 C}{\partial S^2} + VS\sigma_V\rho_{12}\frac{\partial^2 C}{\partial S\partial V} + \sigma_V^2 V\frac{1}{2}\frac{\partial^2 C}{\partial V^2} \\
&+ \lambda_1\int (C(YS,\tau) - C(S,\tau))\, G(Y)\, dY + \lambda_2\int (C(V+y,\tau) - C(V,\tau))\, g(y)\, dy = \frac{\partial C}{\partial \tau}.
\end{aligned} \tag{12}
$$

The call option price is not solved for at the boundary points $V = 0$ and $r = 0$ using (6) and (7). Quadratic extrapolation for obtaining the option values at those points is used. At the point $r = 0$, option values obtained at the points $r = \Delta r,\ r = 2\Delta r, and\ r = 3\Delta r$ by solving the PIDE using Riccati transformation, are used. At the point $V = 0$ option values obtained at the points $V = \Delta V,\ V = 2\Delta V,\ V = 3\Delta V$ are used. The general quadratic extrapolation formula is given by:

$$
f(0) = 3f(\Delta x) - 3f(2\Delta x) + f(3\Delta x).
$$

At $V = V_{max}$ the PIDE becomes:

$$
\begin{aligned}
&(r-q-\lambda_1 k)\, S\frac{\partial C}{\partial S} + (\kappa(\theta - V_{max}) - \lambda_V V_{max})\frac{\partial C}{\partial V} + ((a(b(\tau) - r)) - \lambda_r r)\frac{\partial C}{\partial r} \\
&+ V_{max}S^2\frac{1}{2}\frac{\partial^2 C}{\partial S^2} + \sigma_r^2\frac{1}{2}\frac{\partial^2 C}{\partial r^2} + \sqrt{V_{max}}S\sigma_r\rho_{13}\frac{\partial^2 C}{\partial S\partial r} - rC \\
&+ \lambda_1\int (C(YS,\tau) - C(S,\tau))\, G(Y)\, dY + \lambda_2\int (C(V_{max}+y,\tau) - C(V_{max},\tau))\, g(y)\, dy = \frac{\partial C}{\partial \tau}.
\end{aligned} \tag{13}
$$

At $r = r_{max}$ the PIDE is given as:

$$
\begin{aligned}
&(r_{max}-q-\lambda_1 k)\, S\frac{\partial C}{\partial S} + (\kappa(\theta - V) - \lambda_V V)\frac{\partial C}{\partial V} + ((a(b(\tau) - r_{max})) - \lambda_r r_{max})\frac{\partial C}{\partial r} \\
&+ VS^2\frac{1}{2}\frac{\partial^2 C}{\partial S^2} + \sigma_V^2 V\frac{1}{2}\frac{\partial^2 C}{\partial V^2} + VS\sigma_V\rho_{12}\frac{\partial^2 C}{\partial S\partial V} - r_{max}C \\
&+ \lambda_1\int (C(YS,\tau) - C(S,\tau))\, G(Y)\, dY + \lambda_2\int (C(V+y,\tau) - C(V,\tau))\, g(y)\, dy = \frac{\partial C}{\partial \tau},
\end{aligned} \tag{14}
$$

and for $V = V_{max}$ and $r = r_{max}$ the PIDE is

$$
\begin{aligned}
&(r-q-\lambda_1 k)\, S\frac{\partial C}{\partial S} + (\kappa(\theta - V) - \lambda_V V)\frac{\partial C}{\partial V} + ((a(b(\tau) - r)) - \lambda_r r)\frac{\partial C}{\partial r} - rC \\
&+ \lambda_1\int (C(YS,\tau) - C(S,\tau))\, G(Y)\, dY + \lambda_2\int (C(V+y,\tau) - C(V,\tau))\, g(y)\, dy = \frac{\partial C}{\partial \tau}.
\end{aligned} \tag{15}
$$

Using these boundary conditions together with the PIDE at the non-boundary points, the call option price is obtained. In the next section the MoL is described, which is the method used for numerically solving this problem.

3. Method of Lines (MoL)

MoL is an approximation of one or more partial differential equations with ordinary differential equations in just one of the independent variables, and this approach is discussed in detail by Meyer (2015). The MoL algorithm developed in this paper is an extension of the algorithm for stochastic volatility and stochastic interest rate model proposed by Kang and Meyer (2014), to which jumps to asset returns and volatility are added.

The time dimension is discretised by replacing the partial derivative with respect to time with a backward Euler approximation for the first two time steps, and then the three level backward difference formula for the remainder of the time steps. The partial integro-differential equation is approximated using finite differences. All the derivatives with respect to volatility and interest rate are replaced with finite differences. Integral functions are approximated using Gaussian quadrature, namely, Gauss-Hermite quadrature and Gauss-Laguerre quadrature. The resulting equation is a second order ordinary differential equation, which must be solved at each time step, variance grid point, and interest-rate point.

Within each time step, the second order ordinary differential equation is solved using two-stage iterations. These iterations are done until the price converges to a desired level of accuracy, at which point computations proceed to the next time step. Hence, the MoL approximation would be given by a boundary value problem, together with its boundary conditions. To solve this boundary value problem, it is first transformed into a system of two first-order equations. This system is then solved using the Riccati transformation, which consists of three steps, namely, the forward sweep, followed by the determination of the boundary values at the free boundary, and, finally, the reverse sweep of the appropriate equations. The resulting solution of the reverse sweep gives us the option delta, which is then used to obtain the option values.

3.1. Partial Derivatives Approximation

Let $V_m = m\Delta V$, $r_n = n\Delta r$ and $\tau_l = l\Delta\tau$ for $m = 0, 1, 2, \ldots M$, and $n = 0, 1, 2, \ldots N$ and where $\tau_L = T$. The call option price along the variance line V_m, the interest rate line r_n and the time line τ_l is given by:

$$C\left(\tau_l, S, V_m, r_n\right) = C^l_{m,n}\left(S\right).$$

The option delta at the grid point is given by:

$$V\left(\tau_l, S, V_m, r_n\right) = \frac{\partial C\left(\tau_l, S, V_m, r_n\right)}{\partial S} = V_{m,n}^{l}\left(S\right).$$

The partial derivative discretised with respect to time, $\frac{\partial C}{\partial \tau}$. For the first two time steps, the backward Euler approximation is used:

$$\frac{\partial C}{\partial \tau} = \frac{C_{m,n}^{l} - C_{m,n}^{l-1}}{\Delta \tau}. \tag{16}$$

For subsequent steps, a three-level backward difference formula is used:

$$\frac{\partial C}{\partial \tau} = \frac{3}{2}\frac{C_{m,n}^{l} - C_{m,n}^{l-1}}{\Delta \tau} + \frac{1}{2}\frac{C_{m,n}^{l-1} - C_{m,n}^{l-2}}{\Delta \tau}. \tag{17}$$

Using (16) and (17) together yields a stable numerical method for the solution of the PIDE (Meyer (2015)). The derivative terms are approximated with respect to V and r using finite differences.

$$\frac{\partial C}{\partial V} = \frac{C_{m+1,n}^{l} - C_{m-1,n}^{l}}{2\Delta V}, \quad \frac{\partial C}{\partial r} = \frac{C_{m,n+1}^{l} - C_{m,n-1}^{l}}{2\Delta r},$$

$$\frac{\partial^2 C}{\partial V^2} = \frac{C_{m+1,n}^{l} - 2C_{m,n}^{l} + C_{m-1,n}^{l}}{\left(\Delta V\right)^2}, \quad \frac{\partial^2 C}{\partial r^2} = \frac{C_{m,n+1}^{l} - 2C_{m,n}^{l} + C_{m,n-1}^{l}}{\left(\Delta r\right)^2},$$

$$\frac{\partial^2 C}{\partial S \partial V} = \frac{V_{m+1,n}^{l} - V_{m-1,n}^{l}}{2\Delta V}, \quad \frac{\partial^2 C}{\partial S \partial r} = \frac{V_{m,n+1}^{l} - V_{m,n-1}^{l}}{2\Delta r},$$

$$\frac{\partial^2 C}{\partial V \partial r} = \frac{C_{m+1,n+1}^{l} - C_{m+1,n-1}^{l} + C_{m-1,n+1}^{l} + C_{m-1,n-1}^{l}}{4\Delta V \Delta r}.$$

3.2. Integral Terms Approximation

Gaussian quadrature is used to approximate the integral terms. For an integral function

$$I = \int_a^b f\left(x\right) dx,$$

if $W\left(x\right)$ and an integer N are given, weights w_j and abscissas x_j can be found such that

$$\int_a^b W\left(x\right) f\left(x\right) dx \approx \sum_{j=0}^{N-1} w_j f\left(x_j\right)$$

is exact if $f(x)$ is a polynomial (William H. Press and Flannery (2002)).

The first integral term is

$$\int C(YS,\tau) - C(S,\tau)\, G(Y)\, dY = \int C(YS,\tau)\, G(Y)\, dY - \int C(S,\tau)\, G(Y)\, dY$$

$$= \int C(YS,\tau)\, G(Y)\, dY - C(S,\tau).$$

Following Merton (1976), Y is log-normally distributed and thus $G(Y)$ is given as

$$G(Y) = \frac{1}{Y\delta\sqrt{2\pi}} \exp\left\{ -\frac{\left[\ln Y - \left(\gamma - \frac{\delta^2}{2}\right)\right]^2}{2\delta^2} \right\}, \tag{18}$$

where γ is the mean and δ is the standard deviation. From equation (2), it follows that

$$k = E^{\boldsymbol{Q}}(Y-1) = E^{\boldsymbol{Q}}(Y) - E^{\boldsymbol{Q}}(1) = E^{\boldsymbol{Q}}(Y) - 1 = \exp\left(\left(\gamma - \frac{\delta^2}{2}\right) + \frac{1}{2}\delta^2\right) - 1 = \exp(\gamma) - 1.$$

The remaining integral is approximated using Gauss-Hermite quadrature where

$$W(x) = e^{-x^2} \qquad -\infty < x < \infty.$$

Changing variables in this integral, let $X = \left[\ln Y - \left(\gamma - \frac{\delta^2}{2}\right)\right]$. It is transformed to

$$\int_{-\infty}^{\infty} C(YS,\tau)\, G(Y)\, dY = \frac{1}{\sqrt{\pi}} \int_{-\infty}^{\infty} e^{-X^2} C\left(S \exp\left(\left(\gamma - \frac{\delta^2}{2}\right) + \sqrt{2}\delta X\right), V, r, \tau\right) dX. \tag{19}$$

Using the Gauss-Hermite quadrature formula, equation (19) is discretised,

$$\frac{1}{\sqrt{\pi}} \int_{-\infty}^{\infty} e^{-X^2} C\left(S \exp\left(\left(\gamma - \frac{\delta^2}{2}\right) + \sqrt{2}\delta X\right), V, r, \tau\right) dX,$$

$$= \frac{1}{\sqrt{\pi}} \sum_{j=0}^{J} w_j C_{m,n}\left(S \exp\left(\left(\gamma - \frac{\delta^2}{2}\right) + \sqrt{2}\delta X_j\right)\right),$$

where w_j and X_j are the weights and the abscissas. To obtain the value of the option at the computed point, which might not necessarily lie on the grid, the cubic spline interpolation is used to interpolate between values which lie on the grid. Summing this product gives

the value of the integral at the required point.

The second integral term is

$$\int \left(C\left(V+y,\tau\right)-C\left(V,\tau\right)\right)g\left(y\right)dy.$$

In their "Double Jump" illustrative model, Duffie et al. (2000) assumed that the volatility jump size is exponentially distributed. This ensures that the jumps are always positive. The same assumption of exponential distribution with parameter $\lambda > 0$ is made, regarding the size of the volatility jump. Thus,

$$y \sim \exp\left(\lambda\right),$$

where

$$g\left(y\right) = \lambda e^{-\lambda y}.$$

This integral term is approximated using the Gauss-Laguerre quadrature where

$$W\left(x\right) = x^{\alpha}e^{-x}, \quad 0 < x < \infty. \tag{20}$$

Changing variables in this integral, let

$$X = \lambda y \implies y = \frac{X}{\lambda} \implies dy = \frac{dX}{\lambda}.$$

Substituting back into the equation

$$\int_0^{\infty}\left(C\left(V+y,\tau\right)-C\left(V,\tau\right)\right)g\left(y\right)dy = \int_0^{\infty}C\left(V+y,\tau\right)g\left(y\right)dy - \int_0^{\infty}C\left(V,\tau\right)g\left(y\right)dy,$$

$$= \int_0^{\infty}C\left(V+\frac{X}{\lambda},\tau\right)\lambda e^{-X}\frac{dX}{\lambda} - C\left(V,\tau\right) = \int_0^{\infty}C\left(V+\frac{X}{\lambda},\tau\right)e^{-X}dX - C\left(V,\tau\right).$$

Using the Gauss-Laguerre quadrature formula

$$\int_0^{\infty}C\left(V+\frac{X}{\lambda},\tau\right)e^{-X}dX = \sum_{j=0}^{J}w_j C_{m,n}\left(V+\frac{X_j}{\lambda}\right),$$

where w_j and X_j are the weights and the abscissas. Similarly, as in the previous integral approximation, cubic spline interpolation is used to interpolate between values that lie on the grid to obtain option prices for an asset price, which does not lie on a grid point. Summing this product gives the value of the integral at the required point.

3.3. The Riccati Transformation

From equation (10), the PIDE becomes

$$\begin{aligned}
&(r-q-\lambda_1 k)\,S\frac{\partial C}{\partial S}+(\kappa(\theta-V)-\lambda_V V)\frac{\partial C}{\partial V}+((a(b(\tau)-r))-\lambda_r r)\frac{\partial C}{\partial r}+VS^2\frac{1}{2}\frac{\partial^2 C}{\partial S^2}\\
&+\sigma_V^2 V\frac{1}{2}\frac{\partial^2 C}{\partial V^2}+\sigma_r^2\frac{1}{2}\frac{\partial^2 C}{\partial r^2}+VS\sigma_V\rho_{12}\frac{\partial^2 C}{\partial S\partial V}+\sqrt{V}S\sigma_r\rho_{13}\frac{\partial^2 C}{\partial S\partial r}+\sigma_r\sigma_V\sqrt{V}\rho_{23}\frac{\partial^2 C}{\partial V\partial r}\\
&+\lambda_1\int(C(YS,\tau)-C(S,\tau))\,G(Y)\,dY+\lambda_2\int(C(V+y,\tau)-C(V,\tau))\,g(y)\,dy-rC=\frac{\partial C}{\partial \tau}.
\end{aligned}\tag{21}$$

Substituting for the partial derivatives with respect to time, V and r, together with the mixed partial derivatives using the approximating equations above, an ODE is obtained. For the first two time steps, this is given by:

$$\begin{aligned}
&VS^2\frac{1}{2}\frac{d^2C^l_{m,n}}{dS^2}+(r-q-\lambda_1 k)\,S\frac{dC^l_{m,n}}{dS}-rC^l_{m,n}-\frac{C^l_{m,n}-C^{l-1}_{m,n}}{\Delta\tau}\\
&+(\kappa(\theta-V)-\lambda_V V)\frac{C^l_{m+1,n}-C^l_{m-1,n}}{2\Delta V}+a(b(\tau)-r)\frac{C^l_{m,n+1}-C^l_{m,n-1}}{2\Delta r}\\
&+\sigma_V^2 V\frac{1}{2}\frac{C^l_{m+1,n}-2C^l_{m,n}+C^l_{m-1,n}}{(\Delta V)^2}+\sigma_r^2\frac{1}{2}\frac{C^l_{m,n+1}-2C^l_{m,n}+C^l_{m,n-1}}{(\Delta r)^2}\\
&+VS\sigma_V\rho_{12}\frac{V^l_{m+1,n}-V^l_{m-1,n}}{2\Delta V}+\sqrt{V}S\sigma_r\rho_{13}\frac{V^l_{m,n+1}-V^l_{m,n-1}}{2\Delta r}\\
&+\sigma_r\sigma_V\sqrt{V}\rho_{23}\frac{C^l_{m+1,n+1}-C^l_{m+1,n-1}+C^l_{m-1,n+1}+C^l_{m-1,n-1}}{4\Delta V\Delta r}\\
&+\lambda_1\int(C(YS,\tau)-C(S,\tau))\,G(Y)\,dY+\lambda_2\int(C(V+y,\tau)-C(V,\tau))\,g(y)\,dy=0.
\end{aligned}\tag{22}$$

For subsequent time steps, this becomes:

$$\begin{aligned}
&VS^2\frac{1}{2}\frac{d^2C^l_{m,n}}{dS^2}+(r-q-\lambda_1 k)\,S\frac{dC^l_{m,n}}{dS}-\frac{3}{2}\frac{C^l_{m,n}-C^{l-1}_{m,n}}{\Delta\tau}+\frac{1}{2}\frac{C^{l-1}_{m,n}-C^{l-2}_{m,n}}{\Delta\tau}-rC^l_{m,n}\\
&+(\kappa(\theta-V)-\lambda_V V)\frac{C^l_{m+1,n}-C^l_{m-1,n}}{2\Delta V}+a(b(\tau)-r)\frac{C^l_{m,n+1}-C^l_{m,n-1}}{2\Delta r}\\
&+\sigma_V^2 V\frac{1}{2}\frac{C^l_{m+1,n}-2C^l_{m,n}+C^l_{m-1,n}}{(\Delta V)^2}+\sigma_r^2\frac{1}{2}\frac{C^l_{m,n+1}-2C^l_{m,n}+C^l_{m,n-1}}{(\Delta r)^2}\\
&+VS\sigma_V\rho_{12}\frac{V^l_{m+1,n}-V^l_{m-1,n}}{2\Delta V}+\sqrt{V}S\sigma_r\rho_{13}\frac{V^l_{m,n+1}-V^l_{m,n-1}}{2\Delta r}\\
&+\sigma_r\sigma_V\sqrt{V}\rho_{23}\frac{C^l_{m+1,n+1}-C^l_{m+1,n-1}+C^l_{m-1,n+1}+C^l_{m-1,n-1}}{4\Delta V\Delta r}\\
&+\lambda_1\int(C(YS,\tau)-C(S,\tau))\,G(Y)\,dY+\lambda_2\int(C(V+y,\tau)-C(V,\tau))\,g(y)\,dy=0,
\end{aligned}\tag{23}$$

subject to the boundary conditions:

$$C^l_{m,n}(0) = 0, \quad C^l_{m,n}\left(d^l_{m,n}\right) = d^l_{m,n} - K, \quad \frac{dC^l_{m,n}}{dS}\left(d^l_{m,n}\right) = 1.$$

The boundary conditions discussed in the previous section are imposed. The integrals are approximated using the Gaussian quadrature explained above. To solve equations (22) and (23), each equation is first transformed into two equations of first order.

$$\begin{aligned} \frac{dC^l_{m,n}}{dS} &= V^l_{m,n} \\ \frac{dV^l_{m,n}}{dS} &= A_{m,n}(S)\, C^l_{m,n} + B_{m,n}(S)\, V^l_{m,n} + P^l_{m,n}(S). \end{aligned} \tag{24}$$

This is done by grouping together all the $C^l_{m,n}$ terms, $V^l_{m,n}$ terms and the rest of the terms in $C^l_{m+1,n}$, $C^l_{m-1,n}$ $C^l_{m,n+1}$, $C^l_{m,n-1}$, $V^l_{m+1,n}$, $V^l_{m-1,n}$ $V^l_{m,n+1}$, $V^l_{m,n-1}$ and the integral terms make up the $P^l_{m,n}(S)$ term. This first order system of equations is then solved using a Riccati transformation,

$$C^l_{m,n}(S) = R_{m,n}(S)\, V^l_{m,n}(S) + W^l_{m,n}(S), \tag{25}$$

in which $R_{m,n}(S)$ and $W^l_{m,n}(S)$ are solutions of the initial value problems,

$$\frac{dR_{m,n}}{dS} = 1 - B_{m,n}(S)\, R_{m,n}(S) - A_{m,n}(S)\left(R_{m,n}(S)\right)^2, \qquad R_{m,n}(0) = 0, \tag{26}$$

$$\frac{dW^l_{m,n}}{dS} = -A_{m,n}(S)\, R_{m,n}(S)\, W^l_{m,n} - R_{m,n}(S)\, P^l_{m,n}(S), \qquad W^l_{m,n}(0) = 0. \tag{27}$$

The integration of equation (26) and equation (27) from 0 to S_{max} is called the forward sweep. S_{max} is chosen large enough such that the free boundary point between 0 and S_{max} is obtained. Using each of the $R_{m,n}$ and the $W^l_{m,n}$ values obtained from the integration, the value of the free boundary $S^\bullet$ is between the two consecutive points, where the sign changes on computing values for the following equation:

$$S^\bullet - K - R_{m,n}(S^\bullet) - W^l_{m,n}(S^\bullet) = 0.$$

$d^l_{m,n}$ along the S-grid is defined as the free boundary at the grid point (V_m, r_n, τ_l). In obtaining this free boundary point and the values required for computing the option price

at the free boundary, cubic spline interpolation is used as it is most likely that the free boundary point does not lie on the given grid points. The following equation is integrated for the option delta from $d^l_{m,n}$ to 0. This is known as the backward sweep.

$$\frac{dV^l_{m,n}}{dS} = A_{m,n}(S)\left(R(S)V + W^l_{m,n}(S)\right) + B_{m,n}(S)V + P^l_{m,n}(S), \qquad V^l_{m,n}\left(d^l_{m,n}\right) = 1. \quad (28)$$

At all stages of the calculation the boundary conditions discussed in the previous section are considered. Having obtained the values for $R_{m,n}$, $W^l_{m,n}$ and $V^l_{m,n}$, the option values from the Riccati transformation equation (25) are obtained.

Within each time step, each ordinary differential equation is solved using iterations. Chiarella et al. (2009) look at a similar problem, but with only one jump in the asset dynamics. They use a two stage iterative scheme. In the first stage, they treat the IDEs as ODEs by using $C^{l-1}_{m,n}$ as an initial approximation for $C^l_{m,n}$ in the integral term. The same procedure is followed, the only difference being that there are now two integrals and not one. However, it is the same set of option values that will be used in both integral terms. An initial guess is begun with. For each time period, in each iteration, equations for $m = 1, \ldots, M$ are solved, using the latest values available for $C^l_{m+1,n}$, $C^l_{m-1,n}$ $C^l_{m,n+1}$, $C^l_{m,n-1}$ and $V^l_{m+1,n}$, $V^l_{m-1,n}$ $V^l_{m,n+1}$, $V^l_{m,n-1}$, obtained by using the Riccati transformation. When the difference between the option values for the $(k-1)^{th}$ and the k^{th} iteration is less than 10^{-6}, the iterations are terminated.

In the second stage of iterations, the integral is updated with this new option value and the process is repeated until the price converges at this level, i.e. the difference between the option value in the integral and new computed option value is less than 10^{-6}. The iterations are terminated and the computations are made at the next time step.

4. Numerical Results

In this section, a numerical study is conducted to assess the impact of jumps and the stochastic dynamics of interest rates and volatility on American option prices, and their free boundaries and Greeks. By using the model proposed in Section 2, the MoL is implemented

to price an American call option with strike $K = 100$ maturing in six months on an asset paying a dividend yield of 5%.

To implement the MoL, S, V, r and τ are discretised, in line with the asset dynamics in equation (4). Along the S dimension, a non-uniform mesh is used to handle the lack of smoothness in this problem. There are 50 time steps (L) with the maturity time being $T = 0.5$. $S_{\min} = 0$ and $S_{\max} = 800$ with 50 grid points on $[0, 50]$, 50 grid points on $[50, 100]$, 200 grid points on $[100, 200]$ and 500 grid points on $[200, 800]$, thus totalling 800 grid points. There are 25 variance points with $V_{\min} = 0$ and $V_{\max} = 0.5$ or 50%, and 25 interest rates points with $r_{\min} = 0$ and $r_{\max} =$ 25%. By including jumps, assumptions that the asset price jumps follow a Poisson process and that the volatility jump size is exponentially distributed are made. To approximate the jump integrals, 50 abscissa points are used for the Hermite integration and 5 abscissa points for the Gauss-Laguerre integration. The α of equation (20) is assumed to be 0. The correlation between S and V, $\rho_{12} = -0.5$, and between V and r, ρ_{23}= 0.0. Fama (1981b), Li et al. (2005), Giot (2005) and Fama (1981a) found a significant negative relationship between expected returns and volatility. Cheng et al. (2018) show empirically that, in their data (crude oil futures and USD Treasuries), the correlation between asset volatility and interest rates is almost zero. A similar assumption in this analysis is made. The correlation between S and r (ρ_{13}) can be positive/negative, and it is 0.5 for this analysis. Table 1 presents the parameter values used in the numerical study. Using these parameter values, option prices are computed using the MoL when there are both asset and volatility jumps. [2]

To test the correctness of the MoL implementation, American put prices computed by MoL are compared with prices obtained using the Monte Carlo technique commonly attributed to Longstaff and Schwartz (2001). Several papers provide prices for American put options using the Heston (1993) and Hull and White (1987) model, and which, in particular, use this similar method in their implementation. Some of these results are used for comparison purposes. Samimi et al. (2017) provides tables of values which will be used for comparison.

[2]The parameter values used have been taken from a paper by Chiarella et al. (2009) in which they price American call options with asset dynamics that have stochastic volatility and asset jumps.

Table 1: Parameter values used to compute American call option prices. The Heston (1993) stochastic volatility model and a Hull-White stochastic interest rate model is used. Asset jumps are log-normally distributed, and volatility jumps are exponentially distributed.

Parameters	**Value**	**SV**	**Value**	**SI**	**Value**	**Jumps**	**Value**
T	0.5	θ	0.04	σ_r	0.1	λ_1	5
q	0.05	σ_V	0.4	a	0.3	λ_2	5
K	100	κ	2.0	λ_r	0.0	λ	200
		λ_V	0.0	ρ_{13}	0.5	γ	0.0
		ρ_{12}	-0.5	ρ_{23}	0.0	δ	0.1
				c_1	0.04		
				c_2	0.00		
				c_3	1.0		

In addition to this Python code by Hilpisch (2011)is run in order to obtain the option prices, including the standard errors. Table 2 presents the results for these two different pricing methods for put options.

As indicated in Table 2, the values for the American put option obtained using the MoL are within the Monte Carlo bounds at the 99% confidence interval. The run time for the MoL is more efficient especially when the computation of Greek letters is included, given that MoL computes that as part of the simulations. Chiarella et al. (2009) have demonstrated the time efficiency of the MoL in comparison to component-wise splitting (CS) method and Crank-Nicholson with PSOR method, thus Monte Carlo is only used for comparison purposes.

A sensitivity analysis is conducted next to first examine the impact of stochastic volatility and stochastic interest rates on the shape of the free boundary surfaces in the presence of jumps. Thus, by using jump-diffusion models with jumps in both asset and volatility, an assessment on how the asset prices, stochastic volatility, and stochastic interest rates affect the free boundaries is made. Since this model has non-constant values of volatility and interest rates, an investigation into the effects of changing maximum volatility and maximum interest rate used in the MoL algorithm for discretisation purposes is made, see equation (9).

Table 2: This table presents a comparison of put option prices for two different pricing methods at different interest rate and volatility levels when $S = 100$ using parameter values in Samimi et al. (2017). The American put option prices obtained using the MoL are stated in the 4^{th} column and Monte Carlo prices are in the 5^{th} and 6^{th} columns. LSM1 are prices obtained from Samimi et al. (2017), whilst LSM2 are the prices obtained using the python LSM algorithm by Hilpisch (2011), for 1 million paths and 100 time steps. The standard error given in the 7^{th} column is for the prices obtained using LSM2. The resulting upper and lower price bounds at 95% confidence interval for the LSM2 prices are given in the 8^{th} column and 9^{th} column.

T	**r**	**V**	**MoL**	**LSM1**	**LSM2**	**SE**	**LB**	**UB**
0.2	**0.04**	**0.09**	4.7061	4.689	4.7066	0.0037	4.6993	4.7139
0.2	**0.04**	**0.25**	7.9274	7.907	7.9193	0.0055	7.9085	7.9301
0.2	**0.09**	**0.09**	4.3516	4.337	4.3560	0.0038	4.3486	4.3634
0.2	**0.09**	**0.25**	7.5360	7.511	7.5344	0.0058	7.5230	7.5458
0.3	**0.04**	**0.09**	5.5270	5.490	5.5268	0.0043	5.5184	5.5352
0.3	**0.04**	**0.25**	9.2832	9.245	9.2769	0.0064	9.2644	9.2894

4.1. Sensitivity analysis

The sensitivity of the free boundary is assessed in terms of asset prices, volatility levels, and interest rate levels. Figure 1 displays the impact of interest rates on the free boundary surfaces under two volatility scenarios; a low volatility at 4% and a high volatility environment at 30%. Figure 2 shows the impact of volatility on free boundary surfaces under two interest rates scenarios; a low interest rate at 4% and a high interest rate at 16%. Figure 3 summarises the impact of both volatility and interest rates on the free boundary of an American call option at its maturity date of six months.

As expected, the free boundary value for American call options holds a positive relation with both interest rates and volatility. As interest rates increase, early exercise for a call option is less likely (due to the consequent higher option prices)[3], which drives their free boundaries high. An increase in volatility is expected to increase the free boundary. An increase in volatility increases the time value of the option, thus as the option becomes

[3]Early exercise for a call option occurs when asset value is above the free boundary. The free boundary of a call option increase as interests rates increase, since call options become "better" investments, providing substantially higher returns (compared to positions in the underlying asset), which increases their prices.

more valuable, the free boundary value rises. These effects are more pronounced for longer maturity options and for relatively high levels of volatility and interest rates. For example, an American call option with maturity of 6 months, interest rate at 10% and a volatility of 24% implies a free boundary value of about 290, while for a volatility of 40%, the boundary value is around 307, see Figure 3. The shapes of the free boundary surfaces are similar to the ones produced by models without jumps, see Pantazopoulos et al. (1996) who use front-tracking finite difference methods, Chiarella and Ziogas (2005) who use an iterative numerical integration scheme, Hirsa (2013) who uses the ADI method, and Kang and Meyer (2014) who also use the method of lines for a model with stochastic volatility, etc. The free boundary surfaces are smooth, an advantage of using the MoL. This is a feature that is not shared with other methods, for instance, the finite difference methods, which typically require a smoother (Ikonen and Toivanen (2009)) to be used.

4.1.1. Impact of volatility of volatility

The volatility of financial products is likely to be stochastic. Heston (1993) found that volatility of volatility increases the kurtosis of spot returns. Using a stochastic volatility model, an investigation on the impact of volatility of volatility on the free boundary is made. Figure 6 displays the free boundaries for American call options in the presence of jumps in both asset and volatility dynamics for different vol of vol: 4%, 14%, and 40% when $r = 4\%$ and $V = 4\%$. An increase in the volatility of volatility tends to shift up the free boundary curve, an effect that is more pronounced further from expiry, see Figure 6. Thus, the vol of vol (or kurtosis of returns) has a positive effect on free boundary surfaces, making it less likely for the option to be exercised early.

4.1.2. Impact of volatility of interest rate

Next, an investigation on the effect of increasing the volatility of interest rate on the free boundary is made. Figure 7 displays the free boundaries for American call options in the presence of jumps in both the asset and volatility dynamics for different volatility of interest rates: 8%, 10%, and 12% when $r = 4\%$ and $V = 4\%$. As in the previous analysis, as the volatility of interest rates is increased, the free boundary values also increase, similarly making it less likely for the option holder to exercise the option early. Ho et al. (1997)

illustrate that the value of an American option increases as the volatility of interest rates increase, a change that also depends on asset volatility. Further from expiry, the impact of the interest rate volatility is stronger than the impact of the vol of vol.

4.1.3. Impact of r_{Max} and V_{Max}

As part of the analysis, an investigation on how the choice of r_{Max} and V_{Max} used in the MoL impacts the free boundary values is made. Selection of this value will depend on several factors, including the prevailing market conditions, convergence of values depending on the pricing method being used, the purpose for which the pricing is being done, etc. For instance, a variance that is greater than 100% is a possibility in some markets, especially for small cap stocks or shares from troubled companies (www.macroption.com). Hirsa (2013) discussed the importance of V_{Max} on obtaining good estimates for approximate boundary conditions. Some markets experience negative interest rates; hence, this might also influence the selection of r_{Max} as it will not be as large as when markets experience positive interest rates.

Figure 8a plots the free boundary surfaces for three levels of r_{Max}; $r_{Max} = 0.2$, 0.25, and 0.3. In Figure 8a, as r_{Max} increases, there is a negligible increase in the value of the free boundaries for the same interest rate level. Thus, the selection of r_{Max} does not have a big impact on the resulting free boundary values. An investigation on how the choice of V_{Max} impacts free boundary values is performed. Figure 8b plots the free boundary surfaces for $V_{Max} = 0.5, 0.75, 1.0$.V_{Max} again has negligible impact on the free boundary values, see also Kang and Meyer (2014) for similar conclusions. Thus, the numerical application is robust with regards to the discretisation limits with inconsequential impact on free boundaries.

5. Impact of jumps

To assess the impact of jumps on American call prices, their free boundary surfaces and Greek values, three models are compared: the model with no jumps, the model with jumps in the asset only, and a model with jumps both in asset and volatility. To maintain consistent variance for the three models for comparison, some parameter values have been adjusted as explained next.

Using a spot variance of 4% (or standard deviation of 20%), for the HHWJJ model, the global variance for $\ln S$ is computed by finding the first and second moment of the characteristic function of the model with both jumps and the formula for finding variance being:

$$S^2 = E\left[X^2\right] - E\left[X\right]^2$$

The characteristic function for a 3-D model with no jumps is given by Grzelak et al. (2012), in which asset jump (Kangro et al. (2003)) and volatility jumps (Lutz (2010)) are included. The first and second moments are the first and second derivatives of this characteristic function. For this analysis, the correlation between S and r ρ_{12} is 0.0, the correlation between V and r ρ_{23} is 0.0, and the correlation between S and V ρ_{12} is ± 0.5. There is evidence that the sign of this correlation affects the free boundary differently, see Chiarella et al. (2009). Using these parameter values, the value of the global variance is 24.3% when $\rho_{12} = -0.5$ and 22.1% when $\rho_{12} = 0.5$. This global variance is used as the standard value for the remaining two models (HHWJ and HHW) in which some of the model parameters are changed such that the same global variance is obtained. The difference in the formulation rises from the fact that, for the case with only asset jumps, λ_2 is 0, and when there are no jumps, both λ_1 and λ_2 are zero. In determining these parameter values, which match global variance, an assumption that the spot variance V is equal to the long run mean of V, which is given by θ_V is made, see Chiarella et al. (2009). The interest rate is then adjusted, rounding it off to the nearest percentage, so that, overall, the condition is met. In Table 3, the new parameters for each model are listed, which ensure that this global variance is the same across all models.

5.1. Free boundary surfaces

The impact of asset and volatility jumps on the free boundary is assessed by considering three models: HHW, HHWJ and HHWJJ models. Using the values in Table 1 and Table 3, the free boundary values for the three models are plotted, see Figure 4 for the negative asset volatility correlation case and Figure 5 for the positive asset volatility correlation case. The red line represents the free boundary curve for the HHWJJ model. The black line represents the free boundary curve for the HHWJ model, whilst the blue line is the free boundary curve for the HHW model. The free boundary values for the model with no jumps is lower

Table 3: Parameter values for the models with no jumps and asset jumps, which ensure that the global variance for these models is similar to that of the model with asset and volatility jumps when ρ_{12} is negative (-0.5) and positive (0.5). ρ_{13} and ρ_{23} is 0 in this analysis. $\theta_V = 0.04$, $V = 0.04$, $r = 0.04$ have been selected to be 0.04, 0.04 and 0.04 respectively when there are asset and volatility jumps, giving us a global variance (S^2) of 24.3% (negative correlation) and 22.1% (positive correlation). The rest of the parameters in Table 1 remain the same.

	$\rho_{12} = -0.5$		$\rho_{12} = 0.5$	
Model Parameter	**No Jumps**	**Asset Jumps**	**No Jumps**	**Asset Jump**
V	0.08	0.06	0.08	0.06
θ_V	0.08	0.06	0.08	0.06
r	0.04	0.02	0.05	0.03
λ_1	0.0	0.5	0.0	0.5
λ_2	0.0	0.0	0.0	0.0

than the free boundary values for the models with jumps towards the options expiration. However, as the time to maturity increases, the relation reverses and the free boundaries for the model with no jumps becomes higher than the free boundary for models with jumps. The inclusion of asset jumps and asset-volatility jumps (in comparison to the no jumps case) has a significant impact on free boundaries, especially away from expiry, as it lowers the free boundaries. Thus, in the presence of jumps, the investor is more likely to exercise the option early rather than closer to maturity. This is attributed to the fact that towards expiry, asset and volatility jumps have a direct effect on the option value. When there is sufficient time left to maturity, jumps in asset prices can be balanced out by upcoming offsetting jumps or by long-term mean reverting diffusion.

Further from expiry, adding asset jumps to the HHW model leads to lowering the free boundary. Yet, when volatility jumps are further added to the asset jumps, the free boundary curve elevates, making it less likely for the option holder to exercise the option. Indeed, the HHWJJ model consistently shifts up the free boundary curve, and their difference widens as time-to-maturity increases. In financial terms, this implies that the impact of volatility jumps on the call options prices, when these are added to the asset jumps, is incremental. Note that the global variance between the different model specifications has been held constant. By holding the global variance constant, the variation is entirely allocated in the asset price

dynamics in the models with asset jumps only, while the same variance is distributed in both the asset and volatility dynamics for models with asset and volatility jumps.

The behaviour of the models is similar for positive and negative correlation. The only difference is in the magnitude of the variation between the model with no jumps and the models with jumps, with positive correlation having greater impact on the free boundary surfaces. Similar results were obtained by Chiarella et al. (2009) when contrasting the stochastic volatility model and the stochastic volatility model with jumps for negative and positive correlation. [4] When the correlation is positive, there is a small window period near to expiry in which the model without jumps results in a lower free boundary than the model with asset-volatility jumps.

5.2. American option price

Next, an investigation on the impact of jumps on the American call option price is made, under the assumption of the same global variance across all the three models. Figure 9 shows the differences in the option prices between the three models. The parameter values similar as those used in Figure 4 have been used, where an assumption that the correlation between S and V is -0.5 is made. Negative (positive) differences in the graphs imply that the option price for that particular model (asset jumps or asset-volatility jumps) is greater (lower) than the option price for the no jumps model.

Figure 9 describes the behaviour of the options in terms of moneyness, as jumps are included in the model. When the call option is out-the-money (OTM) or at-the-money (ATM), the option prices for the models with asset jumps and asset volatility jumps are greater than the option price for the no jumps model. Furthermore, the American call price with asset jumps is consistently higher than the American call price with asset-volatility jumps. However, for in-the-money (ITM) call options this relationship reverses and call prices with asset-volatility jumps are worth more than the options with asset jumps. In addition, for ITM options, the prices for models with jumps are worth less than the prices from no jumps models. Like the findings in Section 5.1, when holding global variance constant, options

[4] Yet, these results depend on the quantitative relation between the interest rate and dividend yield in addition to the sign of the mean asset price jump size, see Chiarella and Ziogas (2009).

prices are more sensitive to asset jumps compared to the impact of adding volatility jumps to asset jumps. This may be because, under constant global variance between models, the variation is distributed between asset and volatility (instead of asset dynamics only). There is also possible offsetting in the overall variation in the presence of both asset and volatility jumps. Chiarella et al. (2009) made similar observations when comparing stochastic volatility models with jumps and no jumps. Hence the inclusion of asset jumps and asset-volatility jumps in the model is important when pricing options, as it can lead to the over- or under-estimating of values.

Figure 10 depicts the impact of vol of vol on the American call option price by considering the price differences for the models with no jumps, asset jumps, and asset-volatility jumps for $\rho_{12} = -0.5$. As the vol of vol decreases from 0.4 to 0.1, the option prices for the models with jumps approach the option prices for the no-jumps model.

5.3. Greeks

Another advantage of using the MoL is the fact that Greeks (Delta and Gamma) are computed at the same time as the option values. This helps in terms of time efficiency, in contrast to other methods, which require a separate computation of Greeks. In Figure 11, a comparison of the American call option delta value differences is made for the different models as jumps are included in the model without jumps when $\rho_{12} = -0.5$. The black line represents the model with asset jumps only, and the red line represents the model with asset and volatility jumps. Negative (positive) differences in the graphs imply that the delta for that model (asset jumps or asset and volatility jumps) is greater (lower) than the delta for the pure diffusion model. From Figure 11, including asset jumps increases the delta for OTM options and decreases the delta for ATM and ITM options. For a model with asset-volatility jumps, the delta slightly decreases, although it is still greater than the delta for the no jumps model. When the call option is ITM, the delta for the model with asset jumps is less than the delta for the no-jumps model. Hence, inclusion of asset jumps and inclusion of asset-volatility jumps has a significant impact on the delta of an option, although the impact is slightly less when volatility jumps are added.

6. Conclusion

In this paper, the problem of pricing American call options for an asset for which dynamics incorporate stochastic interest rates of the Hull-White type and with jump-diffusion terms in both asset and volatility dynamics was considered. Asset jumps follow a log-normal distribution and volatility jumps follow an exponential distribution. Using the MoL, free boundaries, option prices, and Greeks are obtained with no extra computational effort. The MoL has been shown to be accurate and efficient. The correctness of MoL implementation has been confirmed through comparison with the Monte Carlo simulation (for demonstration purposes). A sensitivity analysis is performed to gauge the impact of volatility and interest rate parameters on the free boundaries. A further assessment on the impact of jumps on the option prices, the free boundaries, and Greeks is made.

The key findings of the numerical investigations include: The inclusion of asset-volatility jumps has a significant impact on free boundaries, especially away from expiry. Far from expiry, adding asset jumps to the HHW model leads to lowering the free boundary. Yet, when volatility jumps are further added to the asset jumps, the free boundary curve elevates, thus making it less likely for the option to be exercised. The inclusion of an asset-volatility jumps model was found to consistently shift up the free boundary curve, and the difference widens as time-to-maturity increases. The impact of jumps on option prices depends on the moneyness of the option. Option prices for models with both asset and asset volatility jumps are greater than the option price for the no jumps model when the call option is OTM or ATM. The American call prices with asset jumps are consistently higher than the American call price with asset-volatility jumps, a relationship that reverses when call options are ITM. Further, asset jumps increase the delta for OTM options and reduces the delta for ATM and ITM options. On including the volatility jump, the delta slightly decreases, although it is still greater than the delta for the no jumps model. Lastly, the vol of vol and vol of interest rates have a positive effect on free boundary surfaces, whilst rMax and VMax do not have any significant impact on free boundaries.

Possible directions for further research can be models that allow for jumps in interest rate dynamics, given that interest rates may experience sudden fluctuations from time to time. In addition, extensions with more industry relevance can be considered, including applications

to financial products such as pension schemes, which is the topic of the forthcoming research work.

References

Abudy, M., Izhakian, Y., 2013. Pricing stock options with stochastic interest rate. International Journal of Portfolio Analysis and Management 1 (3), 2048–2361.

Adolfsson, T., Chiarella, C., Zioga, A., Ziveyi, J., 2013. Representation and numerical approximation of American option prices under heston stochastic volatility dynamics. Quantitative Finance Research Centre 327, 1–85.

Agarwal, A., Junega, S., Sircar, R., 2016. American options under stochastic volatility: Control variates, maturity randomisation and multiscale asymptotics. Quantitative Finance 16 (1), 17–30.

Amin, K. I., Bodurtha, J. N., 1995. Discrete-time valuation of American options with stochastic interest rates. The Society for Financial Studies 8 (1), 193 – 234.

Amin, K. I., Jarrow, R. A., 1992. Pricing options on risky assets in a stochastic interest rate economy. Mathematical Finance 2 (4), 217 – 237.

Bakshi, G., Cao, C., Chen, Z., 1997. Empirical performance of alternative option pricing models. Journal of Finance 52 (5), 2003 – 2049.

Barone-Adesi, G., Whaley, R. E., 1987. Efficient analytic approximation of American option values. The Journal of Finance (2), 301–320.

Bates, D. S., 1996. Jumps and stochastic volatility: Exchange rate processes implicit in Deutsche Mark options. The Review of Financial Studies 9 (1), 69–107.

Beliaeva, N. A., Nawalkha, S. K., 2010. A simple approach to pricing American options under the Heston stochastic volatility model. The Journal of Derivatives, 25–43.

Black, F., Scholes, M., 1973. The pricing of options and corporate liabilities. Journal of Political Economy 81, 637 – 659.

Boyarchenko, S., Levendorski, S., 2007. American options in levy models with stochastic interest rate of CIR - type. Available at http://ssrn.com/abstract=1032716 or http://dx.doi.org/10.2139/ssrn.1032716, 1–37.

Breeden, D. T., 1976. An intertemporal asset pricing model with stochastic consumption and investment opportunities. Journal of Financial Economics 7, 265 – 296.

Broadie, M., Detemple, J., 1996. American option valuation: New bounds, approximations, and a comparison of existing methods. The Review of Financial Studies 9 (4), 1211–1250.

Broadie, M., Glasserman, P., 1997. Pricing American-style securities using simulation. Journal of Economic Dynamics and Control 21, 1323–1352.

Carriere, J. F., 1996. Valuation of the early-exercise price for options using simulations and nonparametric regression. Insurance: Mathematics and Economics 19, 19–30.

Cheng, B., Nikitopoulos, C. S., Schlögl, E., 2018. Pricing of long-dated commodity derivatives: Do stochastic interest rates matter? Journal of Banking and Finance 95, 148–166.

Chiarella, C., Kang, B., 2011. The evaluation of American compound option prices under stochastic volatility and stochastic interest rates. Journal of Computational Finance 17 (1), 71–92.

Chiarella, C., Kang, B., Meyer, G. H., Ziogas, A., 2009. The evaluation of American option prices under stochastic volatility and jump diffusion dynamics using the Method of Lines. International Journal of Theoretical and Applied Finance 12 (3), 393–425.

Chiarella, C., Nikitopoulos, C. S., Schlögl, E., Yang, H., 2016. Pricing American options under regime switching using Method of Lines. Quantitative Finance Research Centre 368, 1–19.

Chiarella, C., Ziogas, A., 2005. Pricing American options under stochastic volatility. www.semanticsscholar.org, 1–36.

Chiarella, C., Ziogas, A., 2009. American call options under jump-diffusion processes a fourier transform approach. Applied Mathematical Finance 16 (1), 3779.

Chiarella, C., Ziveyi, J., 2011. Two stochastic volatility processes - American option pricing. Quantitative Finance Research Centre 292, 1–73.

Chung, S.-L., 1999. American option valuation under stochastic interest rates. Review of Derivatives Research 3, 283–307.

Clarke, N., Parrott, K., 1999. Multigrid for American option pricing with stochastic volatility. Applied Mathematical Finance 6 (3), 177–195.

Detemple, J., Tian, W., 2002. The valuation of American options for a class of diffusion processes. Management Science 48 (7), 917–937.

Doffou, A., Hilliard, J. E., 2001. Pricing currency options under stochastic interest rates and jump-diffusion processes. The Journal of Financial Research (4), 565–585.

Duffie, D., Pan, J., Singleton, K., 2000. Transform analysis and asset pricing for affine jump-diffusion. Econometrica 68 (6), 1343–1376.

Durhama, G., Park, Y., 2013. Beyond stochastic volatility and jumps in returns and volatility. Journal of Business and Economic Statistics 31 (1), 107–121.

Eraker, B., Johannes, M., Polson, N., 2003. The impact of jumps in volatility and returns. The Journal of Finance (3), 1269–1300.

Fama, E. F., 1981a. Stock returns, expected returns, and real activity. The Journal of Finance 45 (4), 1089–1108.

Fama, E. F., 1981b. Stock returns, real activity, inflation, and money. The American Economic Review 71 (4), 545–565.

Feller, W., 1951. Two singular diffusion problems. Annals of Mathematics 54 (1), 173–182.

Giot, P., 2005. Relationships between implied volatility indices and stock index returns. The Journal of Portfolio Management 31 (3), 92–100.

Grzelak, L. A., Oosterlee, C. W., Weeren, S. V., 2012. Extension of stochastic volatility equity models with the HullWhite interest rate process. Quantitative Finance 12 (1), 89–105.

Guo, S., Grzelak, L. A., Oosterlee, C. W., 2013. Analysis of an affine version of the Heston-Hull-White option pricing partial differential equation. Applied Numerical Mathematics 72, 143–159.

Haentjens, T., int Hout, K. J., 2012. ADI finite difference schemes for the Heston-Hull-White PDE. The Journal of Computational Finance 16, 83–110.

Haentjens, T., int Hout, K. J., 2015. Adi schemes for pricing American options under the Heston model. Applied Mathematical Finance 22 (3), 207–237.

Haowen, F., 2012. European option pricing formula under stochastic interest rates. Progress in Applied Mathematics 4 (1), 14–21.

Heston, S., 1993. A closed-form solution for options with stochastic volatility with applications to bond and currency options. Review of Financial Studies 6 (2), 327–343.

Hilpisch, Y., 2011. Fast monte carlo valuation of american options under stochastic volatility and interest rates. www.archive.euroscipy.org, 1–21.

Hirsa, A., 2013. Computational methods in finance. Chapman and Hall CRC Financial Maths Series.

Ho, T. S., Stapleton, R. C., Subrahmanyam, M. G., 1997. The valuation of american options with stochastic interest rates: A generalization of the Geske - Johnson technique. The Journal of Finance 52 (2), 827 –840.

Hua, J., Shancun, L., Dianyu, S., 2012. Pricing options in a mixed fractional double exponential jump-diffusion model with stochastic volatility and interest rates. Proceeding of 2012 International Conference on Information Management, Innovation Management and Industrial Engineering 3, 1–4.

Hull, J., White, A., 1987. The pricing of options on assets with stochastic volatilities. The Journal of Finance 42 (2), 281–300.

Hull, J., White, A., 1990. Pricing interest-rate-derivative securities. Rev. Finan. Stud. 3, 573592.

Ikonen, S., Toivanen, J., 2009. Operator splitting methods for pricing American options under stochastic volatility. Numer. Math. 113, 299324.

Itkin, A., 2016. Lsv models with stochastic interest rates and correlated jumps. International Journal of Computer Mathematics 94 (7), 1291–1317.

Kang, B., Meyer, G. H., 2014. Pricing an American call under stochastic volatility and interest rates. Nonlinear Economic Dynamics and Financial Modelling - Essays in Honour of Carl Chiarella, 291–314.

Kangro, R., Parna, K., Sepp, A., 2003. Pricing European - style options under jump diffusion processes with stochastic volatility: Applications of Fourier transform. Acta et Commentationes Universitatis Tartuensis de Mathematica 8, 123–133.

Kaushik I. Amin, V. K. N., 1993. Option valuation with systematic stochastic volatility. The Journal of Finance 48 (3), 881–910.

Kou, S., 2002. A jump diffusion model for option pricing. Management Science 48 (8), 1086–1101.

Lamberton, D., Mikou, M., 2008. The critical price for the American put in an exponential levy model. Finance Stoch 12, 561–581.

Lamoureux, C. G., Lastrapes, W. D., 1993. Forecasting stock-return variance: Toward an understanding of stochastic implied volatilities. The Review of Financial Studies 6 (2), 293–326.

Li, Q., Yang, J., Hsiao, C., Chang, Y., 2005. The relationship between stock returns, and volatility in international stock markets. Journal of Banking and Finance 12, 650–665.

Longstaff, F., Schwartz, E., 2001. Valuing American options by simulation: A simple least-squares approach. The Review of Financial Studies 14 (1), 113–147.

Lutz, B., 2010. Pricing of derivatives on mean-reverting assets. Lecture Notes in Economics and Mathematical Systems 630, 1–137.

Makate, N., Sattayantham, P., 2011. Stochastic volatility jump-diffusion model for option pricing. Journal of Mathematical Finance 1, 90–97.

Medvedev, A., Scaillet, O., 2010. Pricing American options under stochastic volatility and stochastic interest rates. Journal of Financial Economics 98, 145–159.

Merton, R. C., 1973. Theory of rational option pricing. The Bell Journal of Economics and Management Science 4 (1), 141–183.

Merton, R. C., 1976. Option pricing when underlying stock returns are discontinous. Journal of Financial Economics 3, 125–144.

Meyer, G. H., 1998. The numerical valuation of options with underlying jumps. Acta Mathematica Universitatis Comenianae 67 (1), 69–82.

Meyer, G. H., 2015. The time-discrete Method of Lines for options and bonds: A PDE approach. World Scientific.

Meyer, G. H., van der Hoek, J., 1997. The evaluation of American options with the Method of Lines. Advances in Futures and Options Research 9, 265–285.

Pan, J., 2002. The jump risk premia implicit in options: Evidence from an integrated time-series study. Journal of Financial Economics 63, 3–50.

Pantazopoulos, K. N., Zhang, S., Houstis, E. N., 1996. Front tracking finite difference methods for the American option valuation problem. Department of Computer Science Technical Reports 1288, 1–15.

Pinkham, S., Sattayatham, P., 2011. European option pricing for a stochastic volatility levy model with stochastic interest rates. Journal of Mathematical Finance 1, 98–108.

Rindell, K., 1995. Pricing of index options when interest rates are stochastic: An empirical test. Journal of Banking & Finance 19, 785–802.

Salmi, S., Toivanen, J., Sydow, L., 2014. An imex-scheme for pricing options under stochastic volatility models with jumps. SIAM Journal on Scientific Computing 36 (5), B817–B834.

Samimi, O., Mardani, Z., Sharafpour, S., 2017. LSM algorithm for pricing American option under Heston-Hull-White's stochastic volatility model. Comput Econ 50, 173–187.

Schobel, R., Zhu, J., 1999. Stochastic volatility with an Omstein - Uhlenbeck process: An extension. European finance review 3 (1), 23–46.

Scott, L. O., 1997. Pricing stock options in a jump-diffusion model with stochastic volatility and interest rates: Applications of Fourier inversion methods. Mathematical Finance 7 (4), 413–424.

Stein, E. M., Stein, J. C., 1991. Stock price distributions with stochastic volatility: An analytic approach. The Review of Financial Studies 4 (4), 727–752.

Sullivan, M. A., 2000. Valuing American put options using Gaussian Quadrature. The Review of Financial Studies 13 (1), 75–94.

Tsitsiklis, J. N., Roy, B. V., 1999. Optimal stopping of Markov processes: Hilbert space theory, approximation algorithms, and an application to pricing high-dimensional financial derivatives. IEEE Transactions of automatic control 44 (10), 1840–1851.

William H. Press, Saul A. Teukolsky, W. T. V., Flannery, B. P., 2002. Numerical recipes in c++: The art of scientific computing. Cambridge University Press.

Zhang, S., Wang, L., 2013. A fast numerical approach to option pricing with stochastic interest rate, stochastic volatility and double jumps. Commun Nonlinear Sci Numer Simulat 18, 1832–1839.

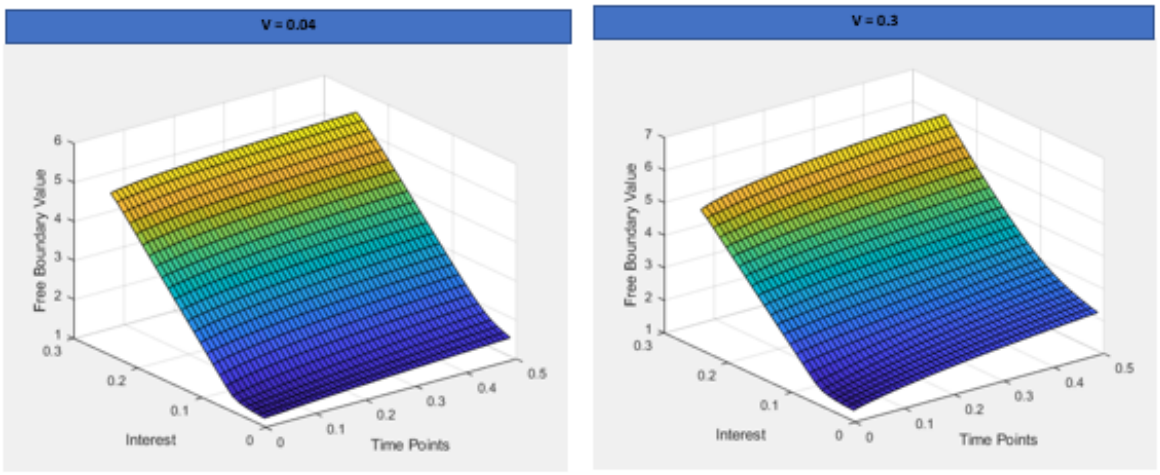

Figure 1: Free boundary surfaces for a six-month American call option obtained using the MoL for a range of interest rates. The left panel considers a low volatility of 4% and the centre panel a high volatility of 30%. The right panel plots the difference between these two sets of free boundary values. The parameter values used are given in Table 1.

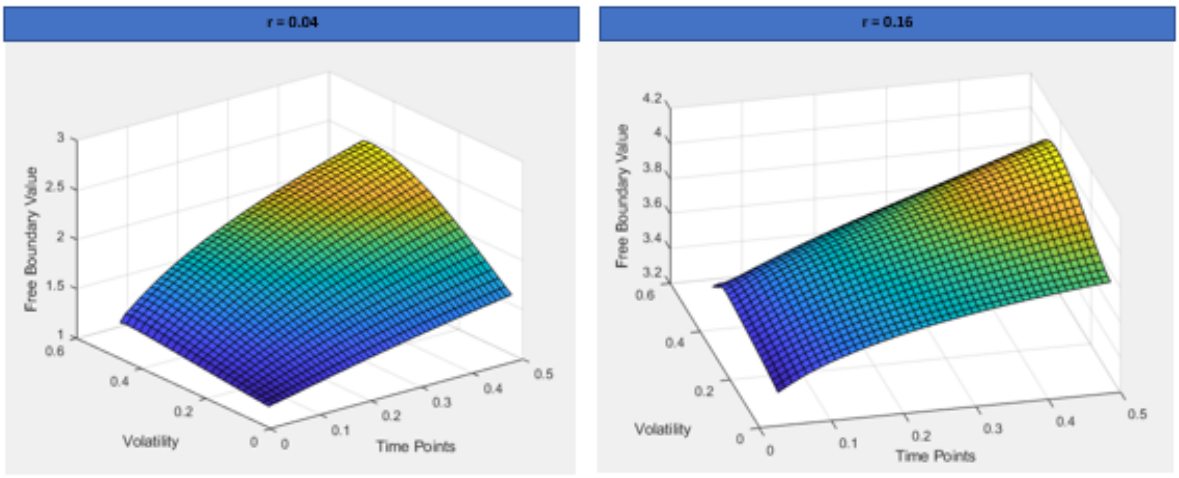

Figure 2: Free boundary surfaces for a six-month American call option obtained using the MoL for a range of volatilities. The left panel considers a low interest rate of 4% and the centre panel a high interest rate of 16%. The right panel plots the difference between these two sets of free boundary values. The parameter values used are given in Table 1.

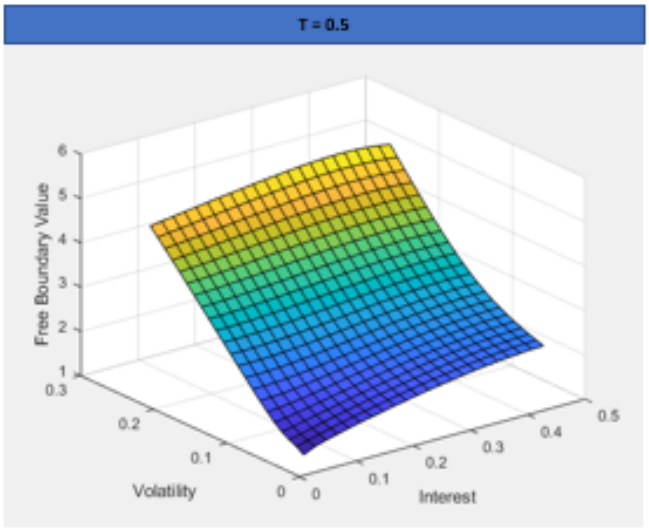

Figure 3: Free boundary surfaces for a six-month American call option for T = 0.5 as interest rates and volatility varies, obtained using the MoL. The parameter values used are given in Table 1.

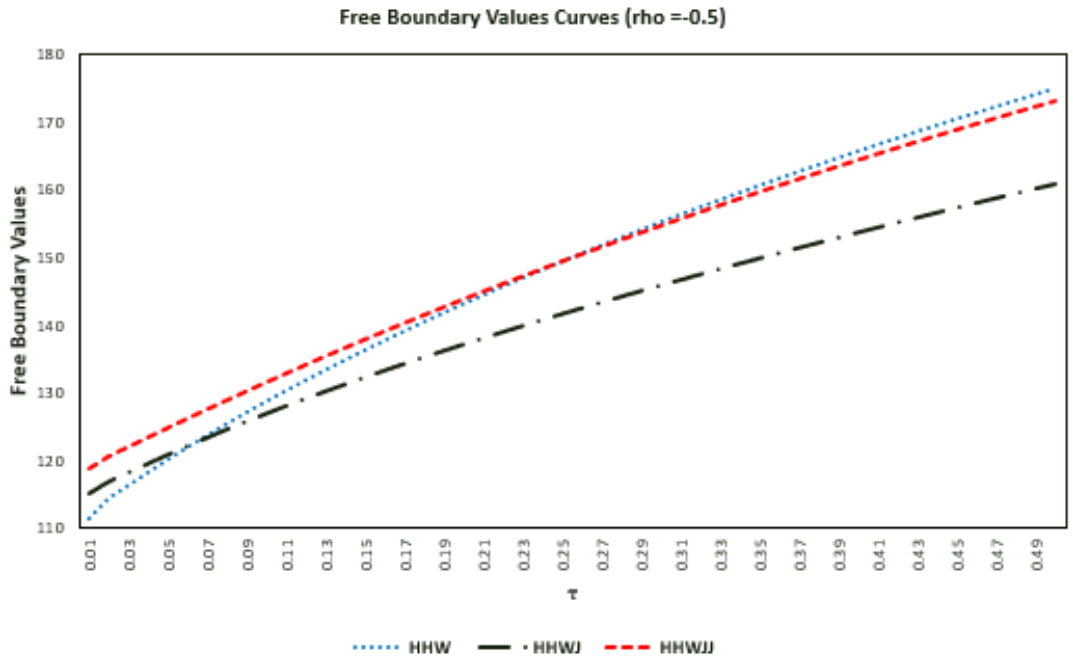

Figure 4: Free boundary surfaces for American call options when $\rho_{12} = -0.5$ under three model specifications: HHW, HHWJ and HHWJJ. The global variance for the three models is 24.3%. The parameter values which ensure the same global variance across all models are given in Table 3, whilst the rest of the parameter values are in Table 1.

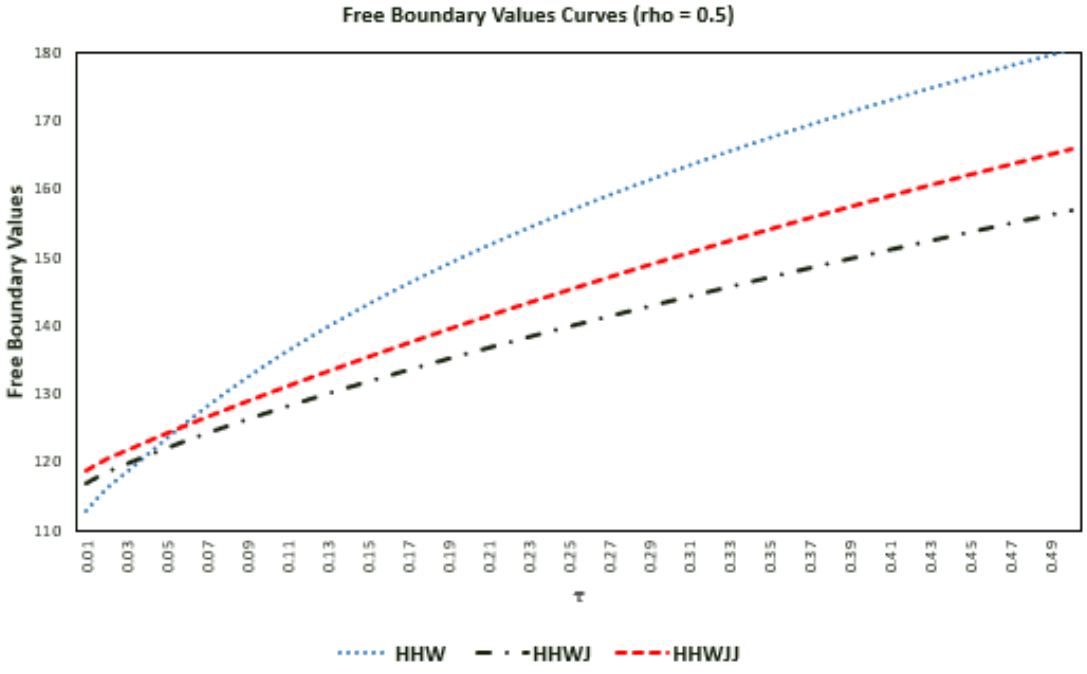

Figure 5: Free boundary surfaces for American call options when $\rho_{12} = 0.5$ under three model specifications: HHW, HHWJ and HHWJJ. The global variance for the three models is 22.25%. The parameter values, which ensure the same global variance across all models are given in Table 3, whilst the rest of the parameter values are in Table 1.

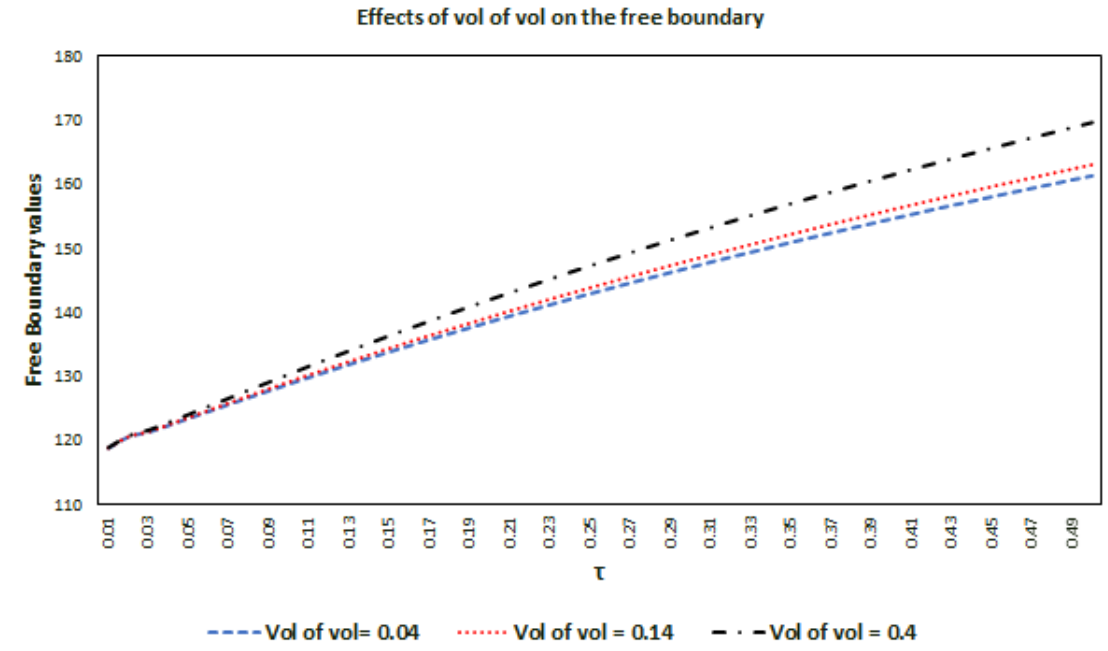

Figure 6: Free boundary surfaces of American call options for different levels of volatility of volatility in the presence of asset volatility jumps when $r = 0.04$ and $V = 0.04$. The parameter values are given in Table 1.

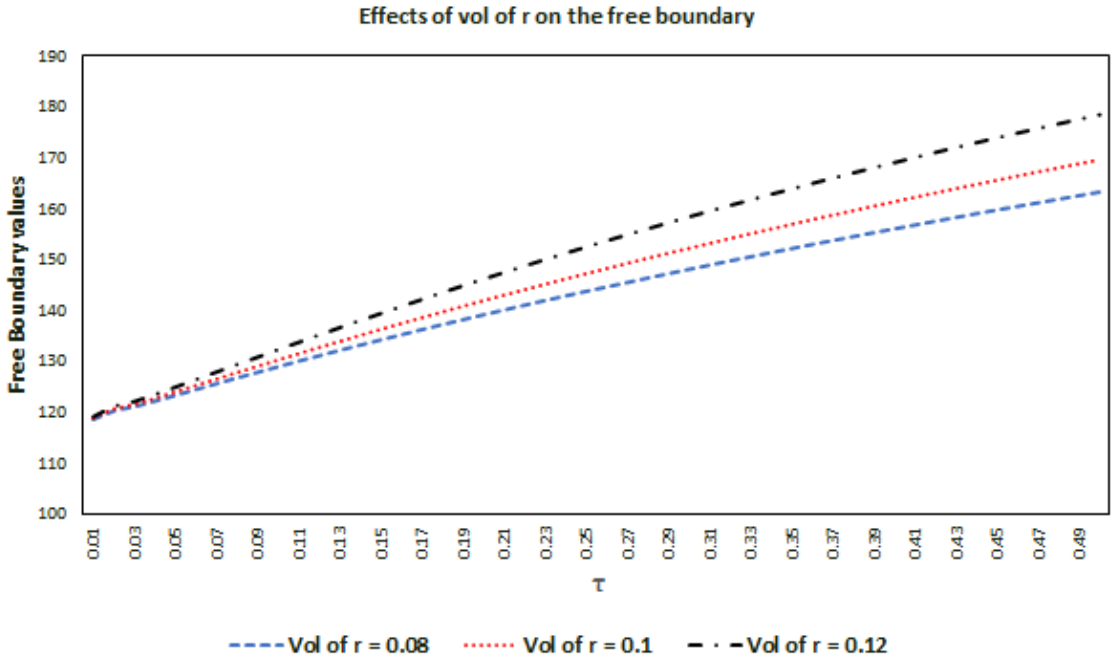

Figure 7: Free boundary surfaces of American call options for different levels of volatility of interest rates in the presence of asset volatility jumps when $r = 0.04$ and $V = 0.04$. The parameter values are given in Table 1.

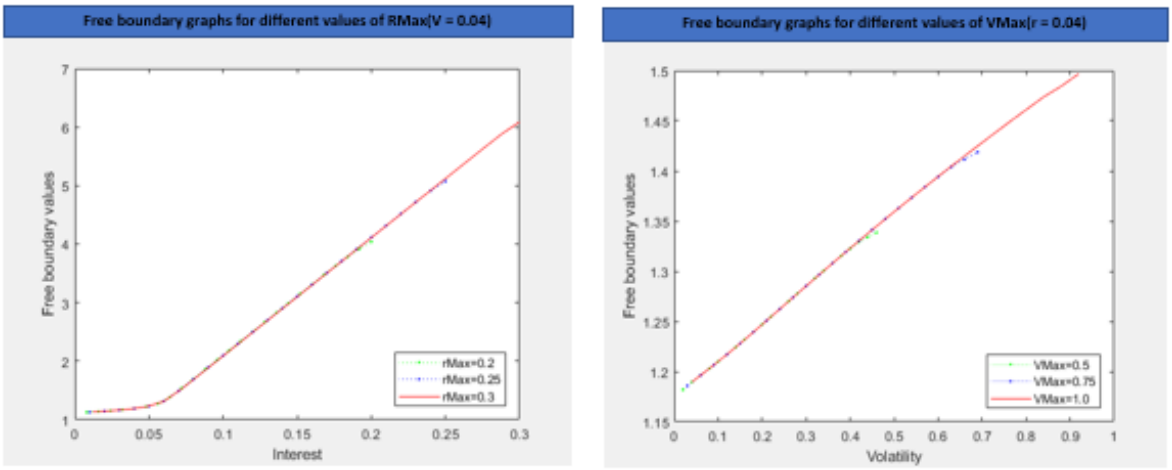

Figure 8: The impact of r_{Max} on the free boundary surfaces of an American call option in the presence of asset volatility jumps when $V = 0.04$ at maturity. The parameter values are given in Table 1.

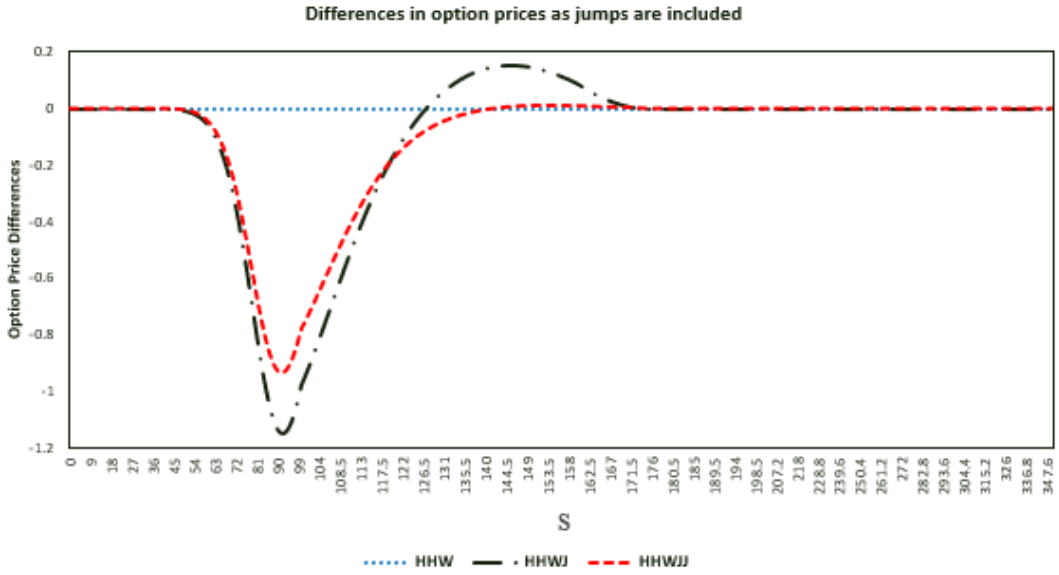

Figure 9: Comparison of American call option price differences for the HHW, HHWJ, and HHWJJ model (for $\rho_{12} = -0.5$). The global variance is 24.3%. The new parameter values, which ensure a similar global variance across all models, are given in Table 3, whilst the rest of the parameter values are in Table 1.

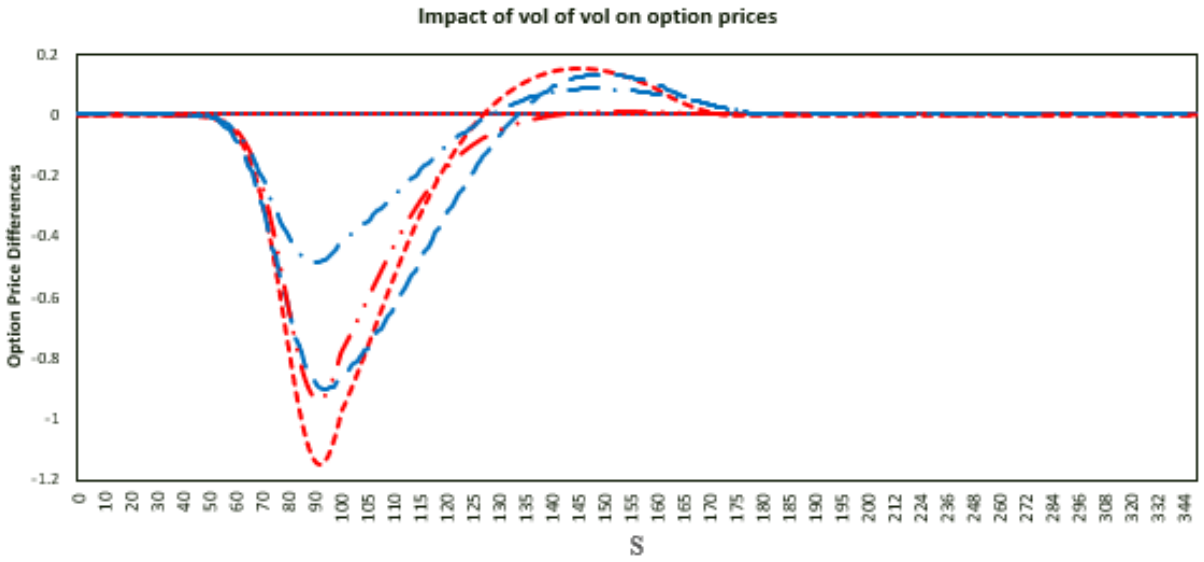

Figure 10: The impact of vol of vol on American call option price by considering the price differences for the HHW, HHWJ, and HHWJJ model (for $\rho_{12} = -0.5$). The global variance is 22.1%. The new parameter values, which ensure a similar global variance across all models are given in Table 3, whilst the rest of the parameter values are in Table 1.

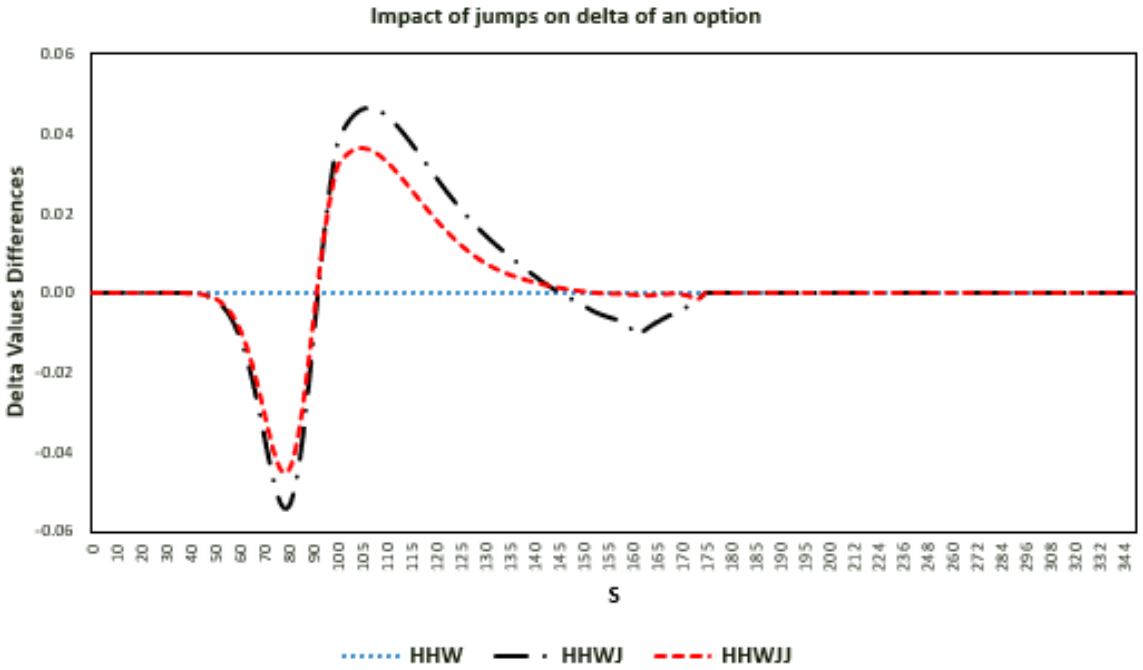

Figure 11: Comparison of American call option delta value differences for the HHW, HHWJ AND HHWJJ model (for $\rho_{12} = -0.5$). The global variance is 24.3%. The new parameter values, which ensure a similar global variance across all models are given in Table 3, whilst the rest of the parameter values are in Table 1.